Journal of Environmental Management 280 (2021) 111707

Contents lists available at ScienceDirect

Journal of Environmental Management

journal homepage: http://www.elsevier.com/locate/jenvman

Research article

Temporal record and spatial distribution of fire foci in State of Minas Gerais, Brazil

Ana Aguiar Real Marinho [a], Givanildo de Gois [b], José Francisco de Oliveira-Júnior [c,d], Washington Luiz Félix Correia Filho [c], Dimas de Barros Santiago [e], Carlos Antonio da Silva Junior [f], Paulo Eduardo Teodoro [g], Amaury de Souza [h], Guilherme Fernando Capristo-Silva [i,*], Welington Kiffer de Freitas [b], Josicléa Pereira Rogério [j]

[a] Department of Engineering Surveying and Cartography, Federal Rural University of Rio de Janeiro (UFRRJ), 23897-000, Seropédica, Rio de Janeiro, Brazil
[b] Postgraduate Program in Environmental Technology – PGTA, Federal Fluminense University (UFF), 27255-250, Volta Redonda, Rio de Janeiro, Brazil
[c] Institute of Atmospheric Sciences (ICAT), Federal University of Alagoas (UFAL), 57072-260, Maceió, Alagoas, Brazil
[d] Postgraduate Program in Biosystems Engineering (PGEB), Federal Fluminense University (UFF), Niterói, Rio de Janeiro, 24220-900, Brazil
[e] Postgraduate Program in Meteorology, Unidade Acadêmica de Ciências Atmosféricas (UACA), Federal University of Campina Grande (UFCG), 58429-140, Campina Grande, Paraíba, Brazil
[f] State University of Mato Grosso (UNEMAT), Department of Geography, Sinop, 78555-000, Mato Grosso, Brazil
[g] Federal University of Mato Grosso do Sul (UFMS), 79560-000, Chapadão do Sul, Mato Grosso do Sul, Brazil
[h] Federal University of Mato Grosso do Sul (UFMS), Mato Grosso do Sul, Brazil
[i] PostGraduate Program in Agronomy (PPGA), Federal University of Mato Grosso (UFMT), Sinop, 78557-267, Mato Grosso, Brazil
[j] Federal University of Rio de Janeiro (UFRJ), COPPE, Rio de Janeiro, Rio de Janeiro, Brazil

ARTICLE INFO

Keywords:
Fires
Burnings
Statistical tests
Vegetation indices
MODIS

ABSTRACT

The objectives of this study are: (i) to evaluate the space-temporal variability of fire foci by environmental satellites, CHIRPS and remote sensing products based on applied statistics, and (ii) to identify the relational pattern between the distribution of fire foci and the environmental, meteorological, and socioeconomic variables in the mesoregions of Minas Gerais (MG) - Brazil. This study used a time series of fire foci from 1998 to 2015 via BDQueimadas. The temporal record of fire foci was evaluated by Mann-Kendall (MK), Pettitt (P), Shapiro-Wilk (SW), and Bartlett (B) tests. The spatial distribution by burned area (MCD64A1-MODIS) and the Kernel density - (radius 20 km) were estimated. The environmental variables analyzed were: rainfall (mm) and maximum temperature (°C), besides proxies to vegetation canopy: NDVI, SAVI, and EVI. PCA was applied to explain the interaction between fire foci and demographic, environmental, and geographical variables for MG. The MK test indicated a significant increasing trend in fire foci in MG. The SW and B tests were significant for non-normality and homogeneity of data. The P test pointed to abrupt changes in the 2001 and 2002 cycles (El Niño and La Niña moderated), which contributes to the annual increase and in winter and spring, which is identified by the Kernel density maps. Burned areas highlighted the northern and northwestern regions of MG, Triângulo Mineiro, Jequitinhonha, and South/Southwest MG, in the 3rd quarter (increased 17%) and the 4th quarter (increased 88%). The PCA resulted in three PCs that explained 71.49% of the total variation. The SAVI was the variable that stood out, with 11.12% of the total variation, followed by Belo Horizonte, the most representative in MG. We emphasize that the applied conceptual theoretical model defined here can act in the environmental management of fire risk. However, public policies should follow the technical-scientific guidelines in the mitigation of the resulting socioeconomic - environmental damages.

1. Introduction

In Brazil, the most traditional way to land clearing, especially when it comes to converting forests into pastures for livestock is by using fire (Caúla et al., 2015; Clemente et al., 2017). Recently, there have been significant increases in the occurrence of burning (resulting from

* Corresponding author. Guilherme Fernando Capristo Silva Universidade Federal de Mato Grosso, 78557-267, Sinop, Mato Grosso, Brazil.
E-mail address: guilhermecapristo51@gmail.com (G.F. Capristo-Silva).

https://doi.org/10.1016/j.jenvman.2020.111707
Received 6 April 2020; Received in revised form 5 October 2020; Accepted 20 November 2020
Available online 23 December 2020

deforestation and logging) and forest fires (degradation or fire scar) in Brazil, and these occurrences often affect protected areas, such as Conservation Units (CU), Permanent Preservation Areas (PPA), Legal Reserves (LR), Indigenous Lands and the biomes (Caúla et al., 2015; Barros Santiago et al., 2019; Lima et al., 2020; Gois et al., 2020; Oliveira Júnior et al., 2020). Burnings are traditional family farming techniques used for cleaning the area for planting temporary crops. They are authorized by the Federal Government (Clemente et al., 2017; Oliveira-Júnior et al., 2017) and generate various economic, ecological, landscape, and social losses to a given area, especially in the protected areas existing in the country (Fiedler et al., 2006; Caúla et al., 2016; Freitas et al., 2020). Burning and forest fires cause the loss of biomass and biodiversity, increased greenhouse gases (GHG) and to a larger extent contributes to climate deregulation at various spatial scales (Dean and Ferro, 1996; Fiedler et al., 2004; Sohngen et al., 2008; Turetsky et al., 2014; Ghazoul et al., 2015; Theisinger and Ratianarivo, 2015; Althoff et al., 2016) Thus, the intensity and frequency of droughts and wildfires are likely to accelerate global warming (Running, 2006; Brando et al., 2019; Boer et al., 2020).

In Brazil, there are public policies (article 41 of the Environmental Crimes Law) to deal with fires in forests and woodlands. The primary public policy was established from the creation of the Action Plan for Prevention and Control of Deforestation in the Legal Amazon (PPCDAm). In order to decentralize the fight against the causes of deforestation and hence burning, which are intrinsic to deforestation, and were limited only to the supervision carried out by environmental agencies, this public policy has positively integrated this oversight into the policies of the Brazilian state. Created in 2004, the Presidential Civil House initially coordinated this intensive action plan until March 2013, when Decree nº. 7,957 transferred this function to the Ministry of Environment (PPCDAm, 2016a; MMA, 2019).

Controlled burning is determined based on categories defined by the federal government. These land categories can be divided into indigenous lands, settlements, protected areas and federal public plots that are mainly used for sustainable development and infrastructure, such as land use planning, construction of inter-municipal and interstate traffic routes, and hydroelectric power stations with their large power transmission lines (PPCDAm, 2016a; PPCDAm, 2016b).

Forest fires can occur through natural, accidental, or criminal intervention (Batista, 2004; MMA, 2019). When their origin is natural, they are caused by a combination of factors such as high temperatures, low air humidity, and atmospheric discharges (Crutzen and Andrea, 1990; Schoennagel et al., 2004; Koutsias et al., 2010; Abatzoglou et al., 2018) and by prolonged drought (Oliveira Júnior et al., 2017; Brando et al., 2019; Boer et al., 2020). Fire is usually a result of anthropogenic activity, and if there is fuel to burn and people to cause ignition, fires will occur (Carmona-Moreno et al., 2005). However, the use of fire helps to promote diversity and natural regeneration, generate open habitats that allow the evolution of plants and animals, pest control among others (Kelly and Brotons, 2017; Pausas and Keeley, 2019). Forest fires, urban fires, and burning contribute significantly to increased air pollution (Donaldson et al., 2000; Donaldson et al., 2001; Sohngen et al., 2008; Silva de Souza et al., 2012), decreased air quality in several urban centers in Brazil (Zeri et al. 2011, 2016) and in the world, especially in the USA, Canada, Australia, Portugal, Spain, Greece and several regions in Asia (Brando et al., 2019; Chuvieco et al., 2019; Bento-Gonçalves and Vieira, 2020; Boer et al., 2020), and even cause damage to the health of the population (Castro et al., 2009; Ribeiro et al., 2013; Tan-Soo and Pattanayak, 2019) and cause huge financial losses (Sayad et al., 2019). Data from the Real-Time Deforestation Detection System (DETER) and the Brazilian Amazonian Satellite Forest Monitoring Program (PRODES) from the National Space Research Institute (INPE) indicated that deforestation increased by 50% in 2019 and the fire focus number increased by approximately 60% compared to the average of the last three years of records, with about 39,000 fires foci in Brazil (INPE, 2019).

Moreover, forest fires contribute to the release of GHG, and mainly carbon dioxide (CO_2) emissions (Moreno et al., 2014; Pausas and Keeley, 2019). Previously, Running (2006) showed that Forest fires add about 3.5×10^{15} g to the atmosphere carbon emissions each year. In Brazil is about 3% of global emissions CO2 (Pereira, 2004; Turetsky et al., 2014). Brazil was sixth in the ranking of the countries that emit most GHG totaling 1,050 million tons of CO_2. Currently, Brazil is the seventh in the ranking of countries that emit greenhouse gases, of which 57.2% are from Land Use, Land Use Change, and Forestry (MCTI, 2016; WRIBrasil, 2016).

With technological advances in recent decades, it is possible to detect the occurrence of forest fires and burns from environmental satellites effectively and at a lower cost compared to other means of surveillance in Brazil (Batista, 2004; Musinsky et al., 2018). Environmental satellites have become a practical and routine alternative in the detection of burned areas, since they provide regional and global coverage of the occurrence of fires (Chuvieco et al., 2019). In Brazil, in the late 1990s, operating system called Burning Database (BDQueimadas) was developed by the Center for Weather Forecasting and Climate Studies (CPTEC) of the National Institute for Space Research (INPE), aiming at monitoring fire foci by environmental satellites from the calculation and prediction of fire risk in vegetation (Setzer and Sismanoglu, 2014; CPTEC, 2018). Fire detection via environmental satellites has been a promising alternative, but there are limitations at the time of detection, as accuracy varies according to cloud coverage (Diniz et al., 2015; Nunes et al., 2015; Caúla et al., 2016; Oliveira Júnior et al., 2017).

The use of environmental satellites in the operational detection of burnings and wildfires in South America has been employed since 1997 from the implementation of the BDQueimadas of the CPTEC/INPE via the Environmental Satellite Division (DSA). BDQueimadas stores several satellite images whose orbits are polar and geostationary obtained from orbital sensors, such as: Advanced Very-High Resolution Radiometer (AVHRR), Imager Radiometer and Vertical Sounder (GOES I-M) – (Setzer and Verstraete, 1994), Along Track Scanning Radiometer (ATSR), Spinning Enhanced Visible and Infrared Imager (SEVIRI), and Moderate Resolution Imaging Spectroradiometer (MODIS) – (Huete et al., 2002; Boschetti et al., 2008; Tomzhinski et al., 2011). The data obtained by BDQueimadas are called fire foci and are available for monthly download. The term “fire foci” is adopted by the official research agency of Brazil, it is defined from pixels (“picture elements”) that present high temperatures, which have the lowest values of gray level in the images of the infrared thermal region band 3 (3.7 μm) of the AVHRR with a minimum area of 1 km^2 are identified (Souza and Stosic, 2011). This term may indicate a burn, small part of a fire or other hot sources, such as reflection of light on the surface of a lake (Tomzhinski et al., 2011) or exposed granites (Nunes et al., 2015; Caúla et al., 2016).

In recent years, some research has been carried out to identify the spatio-temporal pattern of fire foci in Brazilian states such as Rio de Janeiro (Caúla et al., 2016) and Mato Grosso do Sul (Oliveira-Júnior et al., 2020). However, Brazil is a country with continental dimensions, which has 21 states and a Federal District and each state has intrinsic edaphoclimatic characteristics. Therefore, it is necessary more studies to understand the dynamics of fire foci in these states. At the beginning of monitoring, in 1999, the state of Minas Gerais (MG) lost approximately 520 km^2 (52,000 ha) of Federal and State conservation units, and about 900 km^2 (90,000 ha) were cleared for controlled burning, in addition to a significant area of unauthorized fires, such as fires reported in highways margins, in private areas, among others (Lima, 2000; Ribeiro and Figueira, 2011; Arantes Pereira et al., 2012). Even considering the relevance of the theme, few studies were carried out in the state of MG (Lima, 2000; Ribeiro and Figueira, 2011; Arantes Pereira et al., 2012; Camargos et al., 2015), mainly with statistical and geotechnology approaches and by applying mathematical model, which can be reliably and replicable adopted by public management, with the purpose of monitoring and as an auxiliary tool in decision making.

Therefore, the objectives of this study are: (i) to evaluate the space-

temporal variability of fire foci by environmental satellites, CHIRPS and remote sensing products based on applied statistics, and (ii) to identify the relational pattern between the distribution of fire foci and the environmental, meteorological, and socioeconomic variables in the mesoregions of Minas Gerais (MG) – Brazil.

2. Material and methods

2.1. Study area characterization

The state of Minas Gerais (MG) is located in the southeastern region of Brazil, between the latitudes 14° 13' 57" and 22° 55' 47"S, and longitudes 39° 51' 24" and 51° 02' 56"W (Fig. 1), with an area of 582,520 km^2, consisting of 6.9% of national territory subdivided geopolitically into twelve mesoregions (IBGE, 2019). The 12 mesorregions of MG are: 1) – Norte de Minas, 2) – Noroeste de Minas, 3) – Jequitinhonha, 4) – Triângulo Mineiro, 5) – Central Mineira, 6) – Vale do Mucuri, 7) – Oeste de Minas, 8) – Metropolitana de Belo Horizonte, 9) – Vale do Rio Doce, 10) – Sul/Sudoeste de Minas, 11) Campo das Vertentes, and 12) – Zona da Mata.

Besides, there are three biomes in the state of MG: the Cerrado, the Atlantic Forest and Caatinga. It is noteworthy that the three biomes together correspond to 33.8% of the mining territory. The Cerrado has the highest percentage, with 19.94% of the state, a biodiversity-rich biome with more than 6,500 plant species (IEFMG, 2006). Then the Atlantic Forest occupies 10.33% of the territory and is composed of vegetation of Seasonal Deciduous and Semideciduous Forests, Open and Mixed Forest, Dense Ombrophils Forest, and altitude fields (Fundação SOS Mata Atlântica, 2002). Like the Cerrado, the Atlantic Forest is known for being one of the world's richest biodiversity biomes, housing more than 22,039 species of fauna and flora (IEFMG, 2019; IBF, 2019), both of which are included among the 34 conservation hotspot in the world defined by Mittermeier et al. (2005). Caatinga, on the other hand, has the highest species richness among the nuclei of Seasonally Dried Tropical Forests and Shrubs - SDTFS, and in Minas Gerais occupies only 2% of the state's area (Fernandes and Queiroz, 2018).

2.2. Time series of fire foci obtained from environmental satellites

This study used a time series of fire foci from 1998 to 2015. The records came from the BDQueimadas of the Weather Forecasting and Climate Studies Center (CPTEC) and INPE, available at: http://queimadas.dgi.inpe.br/queimadas/bdqueimadas/- (CPTEC, 2018). In one pixel there may be one or several distinct burns, but the indication will be of a single focus (any recorded temperature above 47 °C). If a burn is too extensive, it will be detected in a few neighboring pixels, i.e., several foci will be associated with a single large burn. Such records are obtained from images of the following orbital sensors: **i**) AVHRR/3 of satellites NOAA-15, NOAA-18, NOAA-19, and METOP-B; **ii**) MODIS of orbital platforms TERRA and AQUA; **iii**) VIIRS (Visible Infrared Imaging Radiometer Suite) of satellites NPP (National Polar-orbiting Partnership) versions 375 and SUOMI; and **iv**) satellite images version 13 and 16 of GOES (Geostationary Operational Environmental Satellite) and 3rd generation of MSG (Meteosat Third Generation), that are processed and stored in BDQueimadas (CPTEC, 2018).

2.3. Statistics applied to time series of fire foci

All statistical procedures, such as exploratory and descriptive analysis of fire foci data, were performed in R software version 3.4.2 (R Development Core Team, 2017). Descriptive statistics were used to measure position: mean, median, standard deviation (S), Pearson's asymmetry coefficient (AS), kurtosis (K) and maximum amplitude (A_X). The exploratory analysis also used the boxplot and the frequency density histogram.

In addition to descriptive statistics, Pearson's (r) correlations between the means of the variables evaluated over the time series were estimated. The correlation network was used to graphically express the functional relationship between the estimates of the correlation coefficients between the traits, where the proximity between the nodes (traces) was proportional to the absolute value of the correlation between these nodes. The thickness of the edges was controlled by applying a cutting value of 0.60. Finally, positive correlations were

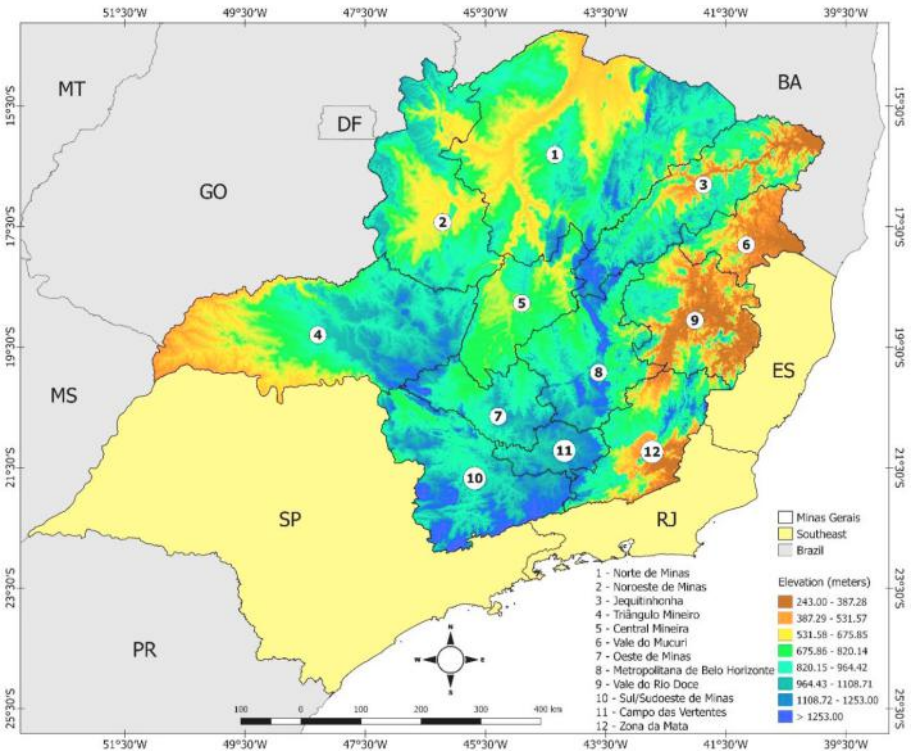

Fig. 1. Map of the State of Minas Gerais, located in the Southeast of Brazil, with twelve mesoregions and hypsometry (m), respectively.

highlighted in green, while negative correlations were represented on a red scale.

To evaluate whether the time series of fire foci follows the criteria of residual normality and homogeneity of variance, the Shapiro-Wilk (Shapiro and Wilk, 1965) and Bartlett (Bartlett, 1937) parametric tests were used, both with a probability at 5%. The SW test analyzes whether the data set follows a normal distribution. The SW test is based on W and is defined by Eq. (1):

$$W = \frac{\left[\sum_{i=1}^{k} a_{n-i+1}\ \left(y_{n-i+1} - y_i\right)\right]^2}{\sum_{i=1}^{n}\left(y_i - \overline{y}\right)^2} = \frac{\left[\sum_{i=1}^{k} a_i\ y_{(i)}\right]^2}{\sum_{i=1}^{n}\left(y_i - \overline{y}\right)^2} \quad (1)$$

Wherein, k = *sample*; i = 1, 2, ……..n is the size sample; y_i is the total value of the sample analyzed; $\overline{y}_i$ is the size mean.

The following hypotheses were adopted:

H_0: Fire foci have a normal (Gaussian) distribution;

H_1: Fire foci do not have a normal (Gaussian) distribution.

For the fire foci to have normal (Gaussian) distribution, the following conditions were considered:

For $W \leq W_{tab}$, H_0 is rejected for p-value <0.05 (significant);

For $W \geq W_{tab}$, H_1 is accepted for p-value > 0.05 (non-significant).

Bartlett's test (1937), B_0, proposed by Snedecor and Cochran (1989), was used to verify the assumption that K samples from a population (N) have equal variances, i.e., homogeneity of variances. This test is expressed by Eq. (2):

$$B_0 = \frac{\left(\sum_{j=1}^{n} n_j - k\right)\ln\frac{1}{\sum_{j=1}^{n} n_j - k}\sum_{i=1}^{k}(n_i - 1)\sum_{j=1}^{n_i}\frac{\left(y_{ij}-\overline{y_i}\right)^2}{n_i - 1} - \sum_{i=1}^{k}\left[(n_i - 1)\ln\sum_{j=1}^{n_i}\frac{\left(y_{ij}-\overline{y_i}\right)^2}{n_i - 1}\right]}{1 + \frac{1}{3(k-1)}\left(\sum_{i=1}^{n}\frac{1}{n_i - 1} - \frac{1}{\sum_{j=1}^{n} n_j - k}\right)} \quad (2)$$

B_0 regarding the hypothesis $H_0 \approx \chi^2_{k-1}$. wherein, n is the number of observations, n_i and k is the number of observations within groups, χ^2_{k-1} is the Chi-square distribution, and B_0 is Bartlett's test statistics.

The following hypotheses were also adopted:

H_0: Fire foci have homogeneous variances;

H_1: Fire foci do not have homogeneous variances.

For fire foci to have heterogeneity or homogeneity, the following conditions are required:

For $B_0 \geq \chi^2_{(1-a,k-1)}$, H_0 is rejected for p-value <0.05 (significant);

For $B_0 \leq \chi^2_{(1-a,k-1)}$, H_1 is accepted for p-value > 0.05 (non-significant).

For evaluating the fire foci trend in MG, the Mann-Kendall (MK) test was applied, because it is assumed the hypothesis of a stable series, where the values occur independently, and the probability disposition must be conserved (simple random series). The tests were also used to analyze the correlation between two variables, that is, for the case of time series. The MK test is described as a time series of x_i of n-terms with a variation ($1 \leq i \leq n$); set to $x = x_1, x_j, \ldots, x_n$ by Eq. (3):

$$S = \sum_{j=i+1}^{n} \mathrm{sgn}\left(x_j - x_i\right) \quad (3)$$

wherein x_j corresponds to the estimated value segment data, n is the length of the time series;

sgn(x) = 1 for $(x_j) - (x_i) > 0$;

sgn(x) = 0 for $(x_j) - (x_i) = 0$; *sgn(x)* = −1 for $(x_j) - (x_i) < 0$.

For series $x = x_1, x_j, \ldots, x_n$ with $n > 4$ according to H_0 hypothesis of no trend, S will show normal distribution with variance *Var(S)* as follows:

$$Var(S) = \frac{n(n-1)(2n+5)}{18} \quad (4)$$

With data replicates, the variance is defined as:

$$Var(S) = \frac{1}{18}\left[n(n-1)(2n+5) - \sum_{p=1}^{g} t_p\left(t_p - 1\right)\ \left(2t_p + 5\right)\right] \quad (5)$$

Wherein, n is the number of observed data; t_p is the number of observed data containing identical values in the set p_{th} and g is the number of sets, including equal values in the p group series. The second term denotes a fit for data.

To test the S significance the bilateral test was used, in which H_0 should be rejected for larger values of Z, which is defined as:

$$MK = \begin{cases} \dfrac{S-1}{\sqrt{Var(S)}} & for \quad S > 0 \\ 0 \quad for \quad S = 0 \\ \dfrac{S+1}{\sqrt{Var(S)}} & for \quad S < 0 \end{cases} \quad (6)$$

Based on the value of Z, it is decided to accept or reject the null hypothesis, so when H_0 is accepted, there is no trend in the time series, and when there is a trend in the time series the null hypothesis is rejected, thereby H_1 is accepted.

In summary:

H_0: Non-significant trend in fire foci time series for p-value > α;

H_1: Significant trend in fire foci time series for p-value < α.

Significance level (α) considered for the test was 5%; thus, for every $p < \alpha$ value, there is a significant trend, while $p > \alpha$ values characterize a non-significant trend.

By means Pettit test (Pettit, 1979), it is possible to verify the year or month in which changes in the variation of segmented data occurred in a historical sequence, where two samples are observed., $X_1, \ldots, X_t$ and $X_{t+1}, \ldots, X_t$, to find out if they belong to the same population (N).

$$U_{t,T} = U_{t-1,T} + \sum_{j=1}^{T} \mathrm{sgn}\ \left(x_i - x_j\right)\ For\ t = 2, \ldots, T \quad (7)$$

wherein; *sgn(x)* = 1 for x > 0; *sgn(x)* = 0 for x = 0; *sgn(x)* = −1 for x < 0.

The statistics for $U_{t,T}$ is counted as 1 < t < T, so the Pettit test k(t) statistic is equivalent to the absolute maximum value of $U_{t,T}$, which is determined as the year or month in which the change occurs, according to Eq. (8):

$$k(t) = \underset{1<t<T}{Max}\left|U_{t,T}\right| \quad (8)$$

It identifies the point on which the abrupt change in the average occurred over a time period and its significant level is given by Eq. (9):

$$p \cong 2\exp\{-6k(t)^2 / (T^3+T^2)\} \quad (9)$$

The abrupt change point is the t where the maximum of $k(t)$ is found, which has the critical values calculated from Eq. (10):

$$k_{crit} = \pm\sqrt{\frac{\ln(p/2)(T^3+T^2)}{6}} \quad (10)$$

2.4. Fire foci mapping via Kernel density

The spatial variability of fire foci in the state of MG was verified from the Kernel density method, performed by Quantum GIS software version 2.18.18 (Qgis Development Team, 2009). The Kernel density method is based on point processes, as in the case of fire foci, and thus can estimate the expected number of events per area unit (Clemente et al., 2017). Mathematical interpolation was adjusted to the two-dimensional function evaluated by the distance of each point to the radius of interest. The Kernel density is obtained by Eq. (11):

$$f(x) = \frac{1}{nh}\sum_{n=1}^{n} K\left(\frac{x - x_i}{h}\right) \quad (11)$$

Wherein K is the Kernel function; h is the search radius; x is the center position of each output raster cell; x_i is the position of the point from the centroid of each polygon, and n is the total number of environmental infractions (Oliveira and De Oliveira, 2017).

In this study, a radius of 20 km was fixed around the fire foci points. However, rays of 5, 10 and 20 km were tested around the points based on the Gualberto (2020) methodology, which tests different rays to identify which of them presents the best visual analysis without prejudicing the quantitative data ranking. It is important to note that the Kernel density estimator is a non-parametric method for estimating density curves, where each observation is weighted by the distance from a central value (Souto Maior and Cândido 2014).

According Medeiros and Câmara (1996), this method can provide a qualitative interpretation of quantitative data for better understanding. The result obtained by Kernel density was classified into three categories: low, medium and high.

The focus density (D) was calculated from Eq. (12):

$$D = \frac{NFCM}{20^2} \quad (12)$$

where, NFCM is the number of fire foci per mesoregion in the state of MG.

2.5. Precipitation spatial analysis via CHIRPS product

In addition to the Kernel density, we used the precipitation product of the 2nd version of the Kernel, the Climate Hazard Group InfRared Precipitation with Station (CHIRPS) (Funk et al., 2015a). The choice of CHIRPS is due to the spatial resolution, which allows to extract the monthly value for each of the 853 municipalities in MG. Furthermore, the accuracy of CHIRPS is an excellent alternative in regions with a lack of rain stations in Brazil (Paredes-Trejo et al., 2017). Other studies point to the effectiveness of CHIRPS, for example, (Funk et al., 2015b; Duan et al., 2016; Katsanos et al., 2016; Bai et al., 2018; Luo et al., 2019; Prakash 2019).

Thus, monthly CHIRPS data for 1998–2015 were used and seasonal (winter and spring), and annual anomalies were extracted with a spatial resolution of 0.05 ° × 0.05 °, for the state of MG, available at ftp://ftp.chg.ucsb.edu/pub/org/chg/products/CHIRPS-2.0 - (Funk et al. 2015a, 2015bbib_Funk_et_al_2015abib_Funk_et_al_2015b).

2.6. Principal Component Analysis (PCA)

After the descriptive analysis and the mapping of heat foci, the Principal Component Analysis (PCA) was applied. The purpose of this analysis was to detect an association between the occurrence of fire foci and meteorological, environmental, and socioeconomic variables in the state of MG. PCA reduces the number of variables from new synthetic variables obtained by the linear combination of the original data, in order to capture the highest variance explained (Preisendorfer 1988; Westerling et al., 2003; Kassomenos and Paschalidou 2017; Kodandapani and Parks 2019; Wilks 2019). However, such a reduction is only possible if these variables are dependent and correlated to each other (Preisendorfer 1988; Wilks 2019). To apply the PCA method the data set quality was initially checked from the Kaiser-Meyer-Olkin test (KMO) (Corrar et al., 2007), obtained by Eq. (13):

$$KMO = \frac{\left(\sum_j\sum_{k\neq j} r_{jk}^2\right)}{\left(\sum_j\sum_{k\neq j} r_{jk}^2 + \sum_j\sum_{k\neq j} p_{jk}^2\right)} \quad (13)$$

Where r is the standard correlation coefficient, p is the standard partial correlation coefficient, and the KMO value ranges from 0 to 1.

According to Corrar et al. (2007), KMO values below 0.5 indicate that the matrix should be discarded, between 0.5 and 0.7 are reasonable, between 0.7 and 0.9 are good, and above 0.9 are considered large. After the previous data evaluation by the KMO test, the PCA was applied. To identify the ideal number of PCs, we used the Kaiser method, which selects eigenvalues higher than 1 ($\lambda > 1$) (Kaiser 1960; Hongyu et al., 2016). Besides the correlation coefficient extracted from each PC, the degree of influence of each PC from its respective factor load (Scores) was also verified.

The PCA was applied to groups of variables: (a) meteorological: Rainfall (R, mm), and Land Surface Temperature during the day (LST-D, °C); (b) vegetation proxies: Normalized Difference Vegetation Index (NDVI), Enhanced Vegetation Index and Soil Adjusted Vegetation Index (SAVI), and Gross Primary Production (GPP, $gC.m^{-2}.\ day^{-1}$); (c) geographical and demographic variables: latitude (°), longitude (°), altitude (m), area of municipality (km^2), population density ($hab.km^{-2}$), municipal human development index (HDI-M).

The NDVI, EVI, SAVI, LST-D, and GPP data were obtained from the MODIS orbital sensor of the TERRA satellite (Rouse et al., 1974; Boschetti et al., 2008). LST-D data was obtained from the MYD11C3 product (Wan et al., 2015) and converted to from K to °C; NDVI and EVI were obtained from the MYD13C2 product (Didan 2015). GPP was obtained from the product MYD17A2 (Running and Zhao 2015), the formulation for obtaining this product is detailed in Souza et al. (2014) The SAVI is obtained by the following expression (Alhammadi and Glenn 2008):

$$SAVI = \frac{NIR - R}{NIR + R + L} * (1 + L) \quad (14)$$

NIR is the near-infrared channel band, R is the red channel band, both obtained from the product MYD13C2. L is the soil reflectance correction factor, for which the value of 0.5 was used. The products have been resized to a spatial resolution grid of 0.05° × 0.05°, and temporal resolution on a monthly scale.

The geographical (coordinates and altitude) and demographic (population density, area of the municipality, and HDI-M) data correspond to the information from each of the 853 municipalities obtained by the 2010 census (IBGE, 2017). In order to carry out the PCA, 2010 was taken as the base year for all variables.

2.7. Burned Area

Fire detection was performed using a contextual algorithm (Giglio et al., 2003) that exploits the high emission of mid-infrared radiation

from fires (Dozier, 1981; Matson and Dozier, 1981). The algorithm examines each pixel of the MODIS swath and ultimately categorizes each pixel into the following classes: missing data, cloud, water, non-fire, fire, or unknown.

The Terra and Aqua combined MCD64A1 Version 6 Burned Area data product is a monthly, global gridded 500-m product containing per-pixel burned-area and quality information. The MCD64A1 burned-area mapping approach employs 500-m MODIS Surface Reflectance imagery coupled with 1-km MODIS active fire observations.

The hybrid algorithm applies dynamic thresholds to composite images generated from a burn-sensitive index that is derived from shortwave MODIS infrared channels 5 and 7, and a measure of temporal texture (i.e. ρ_5-$\rho_7/\rho_5+\rho_7$). The date was then encoded in a single layer of output data in terms of Julian days on which burning occurred (interval 1–366); 0 was assigned to "no burn" pixels and additional special values were assigned to missing data and water grid cells. We sought to calculate the burned areas for the Amazon basin (1-365 Julian days). The burned area data will be calculated only for the years identified by the Pettitt test (Fig. 6 and Table 1) from the rainfall anomalies via CHIRPS product.

All statistical, geotechnology, and free software tools (R Development Core Team., 2011), together with the available data (fire foci, CHIRPS, and MODIS products) are in the flowchart summarizing the methodology used in the study (Fig. 2).

3. Results and discussion

3.1. Statistical tests and statistical inference

Analysis of the *SW* and *B* tests (Table 1) applied to the time series of fire foci in the state of MG showed that the tests were significant for normality and homogeneity of variance at 5% probability level. Therefore, we reject hypothesis H_0 that the fire foci time series has a normal and homogeneous distribution. It is noteworthy that there was a significant growth trend ($z > \alpha$) in the fire foci recorded in the state of MG, according to the MK test for p-value <0.05 probability, followed by the magnitude of (S_{en}) of 0.69. The magnitude-increasing effect of fire foci differs from that found in probability, and this is one of the flaws in decision-making models. This growing trend in the number of fire foci in the state may be related to the recurrent drought periods and the severity of droughts in recent years in various regions of the state (Minuzzi et al., 2007; Reboita et al. 2010, 2015bib_Reboita_et_al_2010bib_Reboita_et_al_2015), similar result based on MK test was obtained for the biomes (Pantanal, Cerrado, and Mata Atlantica) existing in the state of Mato Grosso do Sul (MS), where there was a positive increase trend of fire foci associated with periods of drought and extensive agriculture (Oliveira-Júnior et al., 2020). Moreover, the change in orbital sensors along with the time series (Caúla et al., 2015) and the significant increase in BDQueimadas environmental satellite network from the 2010s may help regarding new findings (Caúla et al., 2016).

3.2. Descriptive and exploratory statistics

According to the exploratory and descriptive statistics (Table 2), it is verified that during the study period, there were a total of 602,226 fire foci throughout the state of MG. Descriptive statistics indicated that the mean and standard deviation was 33,457.00 ± 5,723.67 fire foci, followed by the median of 28,187 fire foci, and the mode of 4,799 fire foci in the state of MG. The maximum and minimum values were identified in the mesoregions of Northern Minas (24.958 fire foci year^{-1}), Jequitinhonha (18,174 fire foci year^{-1}), and Campos dos Vertentes (36 fire foci. year^{-1}), respectively. The highest standard deviation was observed in the North of Minas, with 7.078,51 fire foci year^{-1}. The North, Jequitinhonha, and Triângulo Mineiro mesoregions stand out in the total accumulated and in the percentage, which together corresponds to 57.96% fire foci in the state of MG (see Table 3).

Regarding the coefficient of variation (CV%), the highest values occurred in the mesoregions of Belo Horizonte (109.75%), Vale do Mucuri (126.77%), and Vale do Rio Doce (118.14%), all located in the southeast of the state and characterized by high population density, and high industrial and agricultural activity (IBGE, 2017). All mesoregions of the state had a positive AS coefficient; regarding the kurtosis coefficient, all were categorized as Platykurtic, except the Vale do Mucuri mesoregion (Leptokurtic). Conversely, Gois et al. (2020) found for the state of Rio de Janeiro (SRJ) a predominance of Leptokurtic distributions ($K > 3$, sharpest curve) greater than platykurtic distributions ($K < 3$, a more flattened curve).

It is observed that the mean value was higher than the median due to the presence of outliers in the data, followed by the high discrepancy between minimum and maximum verified by the high value of the standard deviation. The outliers identified in the fire foci time series are possibly justified by the change in orbital sensors over time. For example, the sensor used previously was AVHRR, then the MODIS sensor was adopted, and now VIIRS is used, followed by the entry of new reference satellites adopted by BDQueimadas. In addition to these factors, the interannual and intraseasonal variability of meteorological systems acting on the Southeast (Reboita et al., 2010; Caúla et al., 2015; Clemente et al., 2017; Mendes et al., 2019) interfere with rainfall, wind, atmospheric stability, temperature and air humidity patterns, which are the variables responsible for the dynamics of forest fires and burning (Batista, 2003; Van Der Werf et al., 2008).

Based on the histogram of normalized fire foci (Fig. 3), it can be seen that the tail of the normal distribution curve for the MG state is longer on the right, indicating that the fire foci time series is asymmetric positive (Meira-Neto et al., 2005) and does not have a normal distribution. Regarding the Jequitinhonha and Triângulo Mineiro mesoregions, the fire foci time series of each mesoregion are close to normal distributions. The exception occurred in the Northern Minas mesoregion, which despite having similar characteristics to the state of MG, it is worth mentioning the density equal to 1.

The absolute frequency distribution of fire foci in MG (Fig. 4) showed an inverted "J" format similar to the diameter distribution (Meira-Neto et al., 2005). Fig. 4 shows the diameter distribution of the fire foci raised in the study and clustered into classes with 1,000 fire foci intervals. The inverted "J" shape presents a pattern where it is observed that the higher the frequency, the smaller the trend of many fire foci; however, it is observed that in the higher frequencies, a larger number of fire foci are also verified. In the class from 9,000 to 10,000 fire foci, the curve has a discontinuity, probably due to greater intervention in the area. It is also noteworthy that this type of size structure when referring to Land Use Change, it is often interpreted as an indicator of population stability or increase, or capacity for self-regeneration and reproduction under the canopy, while bell-shaped structures indicate species that do not often reproduce under the canopy and require clearing for regeneration to occur (Meira and Cabacinha, 2016).

Specifically, there is a higher frequency of fire foci in the first

Table 1
Results of the Shapiro-Wilks, Bartlett, Mann-Kendall, and Pettitt tests applied to the fire foci time series in the state of Minas Gerais, from 1998 to 2015.

Shapiro-Wilks		Bartlett		Mann-Kendall			Pettitt	
W	p-value	χ^2	p-value	*Z*	S_{en}	p-value	Kcritical	p-value
0.5196	2.20×10^{-16}	620.61	2.20×10^{-16}	0.686	0.69	8.17×10^{-5}	55.4	0.0336

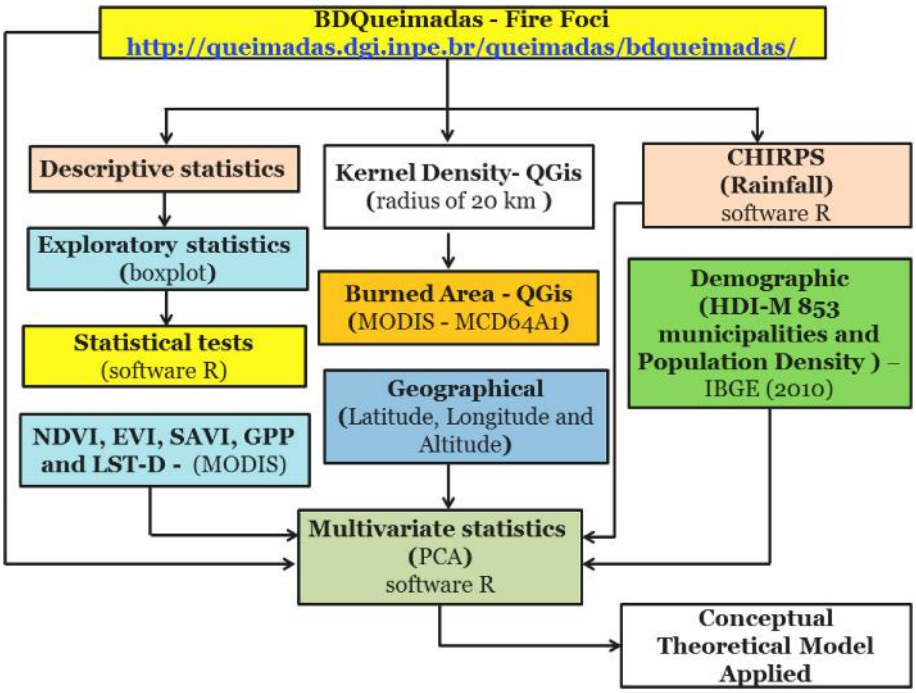

Fig. 2. Flowchart of the methodology applied in the study.

Table 2
Descriptive statistics (mean, median, mode, minimum, maximum, amplitude, upper and lower limits) applied to fire foci for the twelve mesoregions of the state of Minas Gerais, from 1998 to 2015.

Mesorregions	Total Accumulated	Total Percentage (%)	Mean	Median	Mode	Minimum	Maximum	Amplitude	Upper Limit	Lower Limit
North	181270****	30.10****	10070.56	9836.50	1385.00	1148	24958	23810	−11347.50	29832.50
Jequitinhonha	85817****	14.25****	4767.61	3736.50	559.00	396	18174	17778	−4390.38	12510.63
Zona da Mata	15637	2.60	868.72	568.50	104.00	104	3511	3407	−942.63	2526.38
Vale do Rio doce	43880	7.29	2437.78	1417.00	728.00	395	11246	10851	−1632.75	5265.25
Vale do Mucuri	19231	3.19	1068.39	694.00	260.00	81	5574	5493	−464.00	1850.00
Triângulo Mineiro	81939***	13.61****	4552.17	3995.50	508.00	508	9894	9386	−2309.75	11426.25
South-Southwest	24017	3.99	1334.28	942.50	150.00	150	3797	3647	−1485.88	3909.13
West	17207	2.86	955.94	837.50	147.00	147	2519	2372	−1387.13	3157.88
Northwest	65229	10.83	3623.83	3466.50	557.00	557	8773	8216	−4755.13	11507.88
Belo Horizonte	35694	5.93	1983.00	1124.50	172.00	168	7978	7810	−2221.25	5532.75
Central	24703	4.10	1372.39	1201.50	193.00	137	2719	2582	−1717.88	4619.13
Campos das Vertentes	7602	1.26	422.33	366.50	36.00	36	1290	1254	−435.38	1195.63
TOTAL	602226	100	33457.00	28187.00	4799.00					

Table 3
Descriptive statistics (Sample variation, asymmetry, kurtosis coefficients, sample standard deviation, standard error, quartile, and Interquantilic amplitude) applied to fire foci for the twelve mesoregions of the state of Minas Gerais, from 1998 to 2015.

Mesorregions	Coefficients					Sample Standard Deviation	Standard Error	Quartile		Interquantilic Amplitude
	Sample variation (%)		Assimetry		Kurtosis (K)			Lower	Upper	
North	70.29	0.43	+	−0.89	Platykurtic	7078.51	1668.42	4095.00	14390.00	10295.00
Jequitinhonha	90.96	1.52	+	2.44	Platykurtic	4336.61	1022.15	1947.50	6172.75	4225.25
Zona da Mata	95.97	1.72	+	2.86	Platykurtic	833.74	196.51	358.25	1225.50	867.25
Vale do Rio doce	118.14	1.97	+	2.88	Platykurtic	2880.00	678.82	954.00	2678.50	1724.50
Vale do Mucuri	126.77	2.17	+	4.19	Leptokurtic	1354.42	319.24	403.75	982.25	578.50
Triângulo Mineiro	65.12	0.39	+	−1.04	Platykurtic	2964.28	698.69	2841.25	6275.25	3434.00
South-Southwest	78.81	0.86	+	−0.46	Platykurtic	1051.49	247.84	537.25	1886.00	1348.75
West	76.82	0.65	+	−0.83	Platykurtic	734.31	173.08	317.25	1453.50	1136.25
Northwest	67.17	0.35	+	−1.07	Platykurtic	2433.99	573.70	1343.50	5409.25	4065.75
Belo Horizonte	109.75	1.56	+	1.42	Platykurtic	2176.27	512.95	686.50	2625.00	1938.50
Central	65.53	0.20	+	−1.54	Platykurtic	899.35	211.98	658.50	2242.75	1584.25
Campos das Vertentes	73.28	1.03	+	0.94	Platykurtic	309.50	72.95	176.25	584.00	407.75

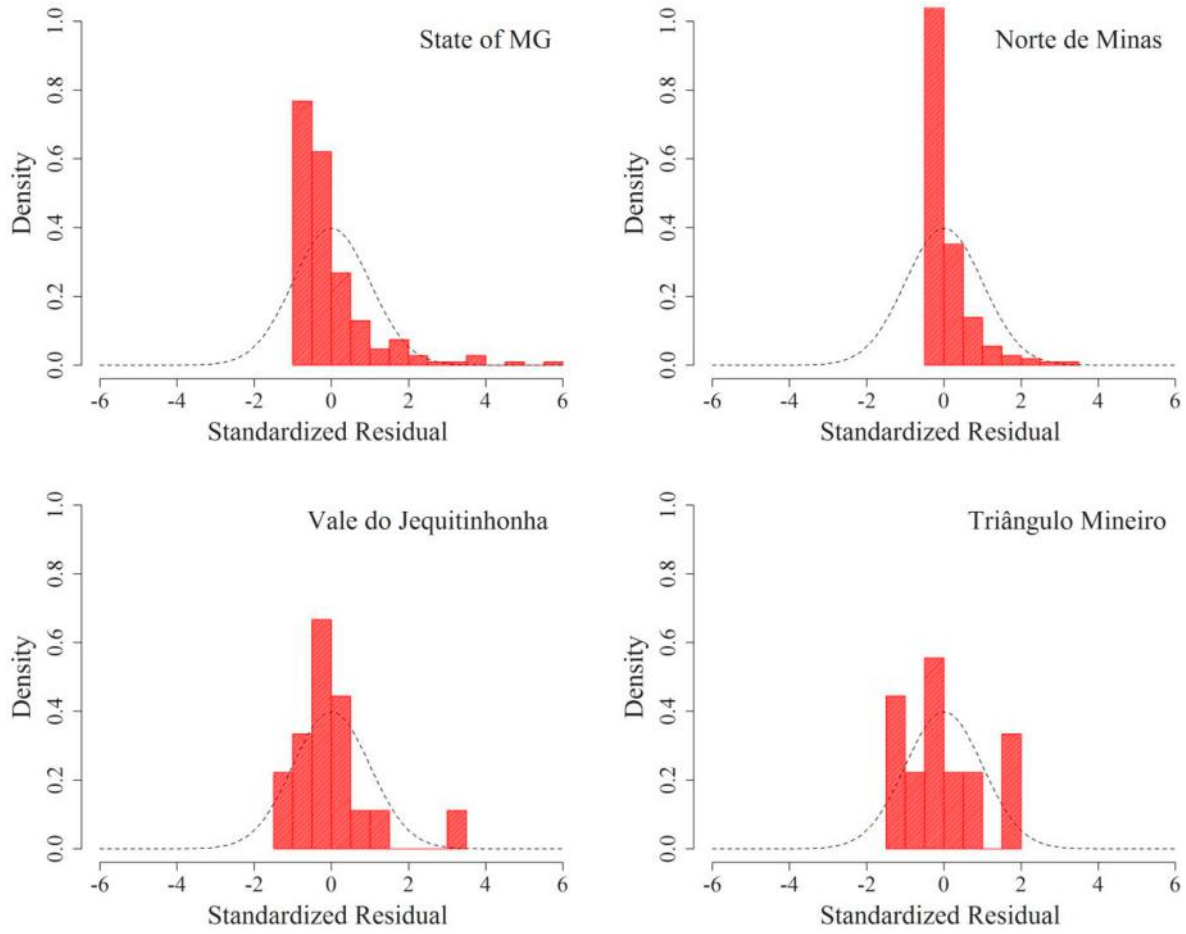

Fig. 3. Density histogram versus standard residue of normalized fire foci in the state of Minas Gerais, North of Minas Gerais, Jequitinhonha Valley and Triângulo Mineiro from 1998 to 2015.

confidence interval, from 0 to 25,000 fire foci in MG during the study period. It is noteworthy that such concentration in this confidence interval is also associated with the evolution of orbital sensors, the implemented algorithms, the current number of environmental satellites and, finally, the types of satellites in BDQueimadas the network (geostationary and heliosynchronous) – (Antunes, 2000; Caúla et al., 2015; Clemente et al., 2017). In the Jequitinhonha mesoregion, most fire foci are concentrated from 0 to 10,000, with the exception of the 20,000 fire foci class, opposite situation to the North Minas mesoregion, which presents fire foci variability across all classes. The Triângulo Mineiro mesoregion presented the lowest occurrence among all mesoregions and in relation to the state of MG.

Fig. 5 shows a variability pattern of fire foci in the state of MG, where the most substantial records occurred from August to October. Our findings corroborate the results found by Caúla et al. (2015) when it assessed fire foci for Brazil, which may be related to the transition between dry and rainy periods (Coutinho, 1990). Thus, the vegetation is more vulnerable to fire action due to the low humidity and the absence of rain in these months (Van Der Werf et al., 2008).

3.3. Pettit test and Kernel density

Trend detection in time series is crucial for good practices and natural resource management and can be done through non-parametric statistical tests such as the Pettit test (Table 1), which pointed to an abrupt change in fire foci time series in the year 2001 and 2002 (Fig. 6), motivated by the abrupt growth of fires. Previously, Moreno et al. (2014) used the Pettitt test and confirmed significant changes in the number of fires and burned areas during the vegetative and non-vegetative periods in all regions of Spain in 1970, followed by the Northern and Interior regions in 1980 and the Mediterranean in 1990. Lima et al. (2020) based on Pettitt's test also showed a significant increase ($p \leq 0.05$) in fire foci for most Indigenous Lands in the state of Mato Grosso, starting in 2009. It is noteworthy that this year is part of the 2001/2002 cycle (El Niño and La Niña moderate), which contributes to the annual increase of fire foci, and the same condition was previously identified by Clemente et al. (2017) and Freitas et al. (2020) in the SRJ. Previously, Carmona-Moreno et al. (2005) identified the global scale influence of ENSO on fire activity over a 17-year period. Recently, Lima et al. (2020) identified a significant increase in fire foci in Indigenous Lands in the state of MG in 2009, categorized as El Niño moderate. This year there was below the average rainfall, followed by prolonged droughts and positive air temperature anomalies from January to August (Climanálise, 2020).

It cannot be ruled out that the increased occurrences are possibly related to the change of the reference satellite (NOAA-12). Besides, the change of the AQUA (moving at 4:00 am and 5:00 pm Greenwich Mean Time - GMT) and EARTH (moving at 3:00 am and 2:00 pm) - (INPE, 2017) satellites may also have contributed to the increased records. Added to the improvement of satellites/orbital sensors, there is the influence of rainfall deficit in much of the Southeast Region (CPTEC, 2017).

According to the Kernel Density Map (Figs. 7 and 8), it is found that the low category ranged from 0 to 16 fire foci, followed by the medium category with 17–48 fire foci, and finally the high category with 48–64 fire foci per unit of area. There is an occurrence of the high category in

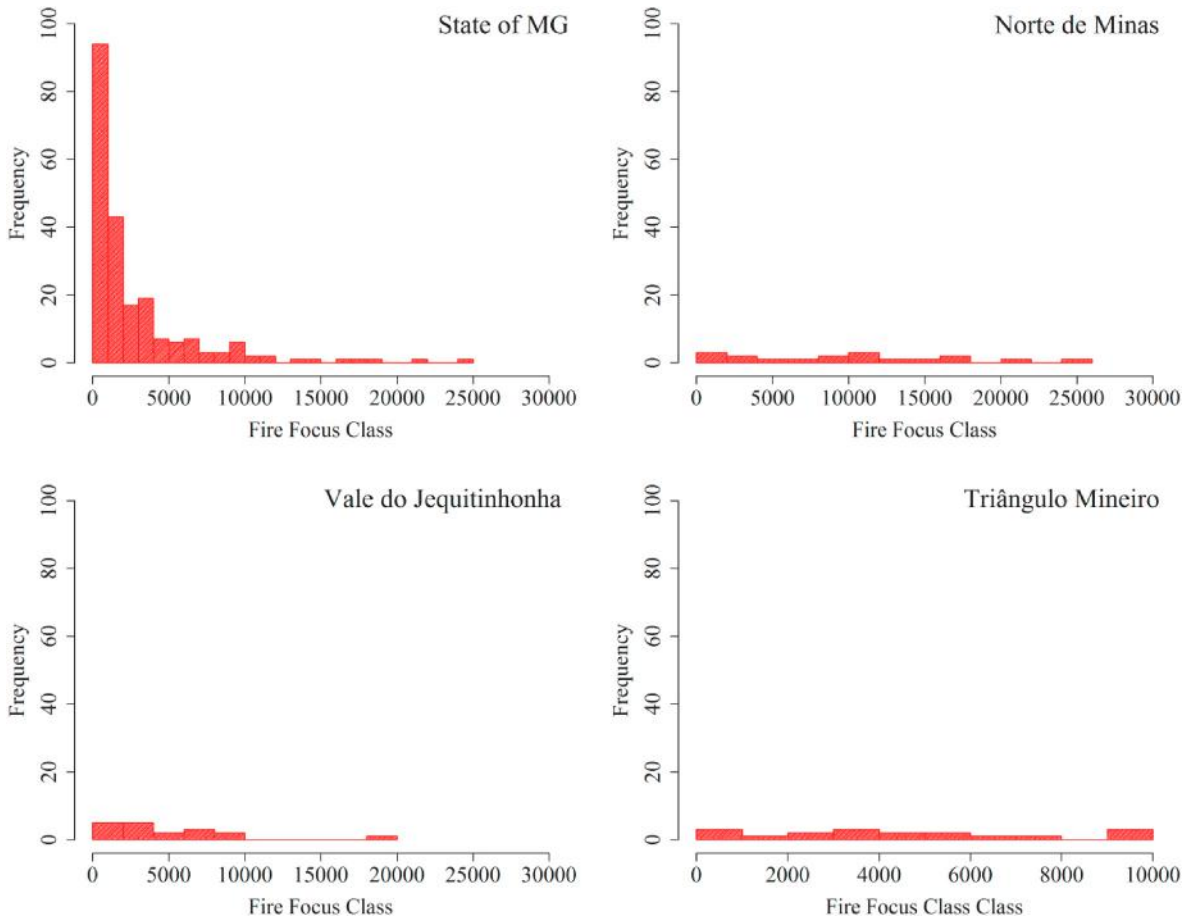

Fig. 4. Histogram of the absolute frequencies of fire foci in the state of Minas Gerais, North of Minas, Jequitinhonha Valley and Triângulo Mineiro from 1998 to 2015.

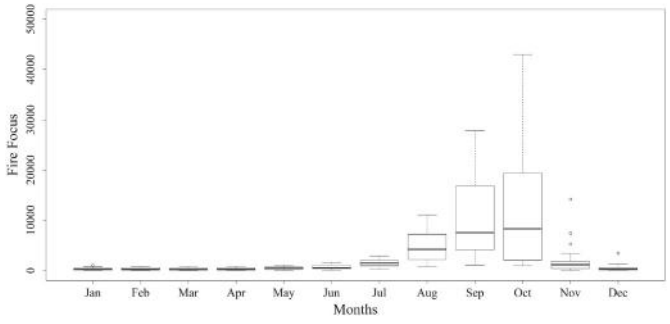

Fig. 5. Monthly boxplot of fire foci in the state of Minas Gerais in the period 1998–2015.

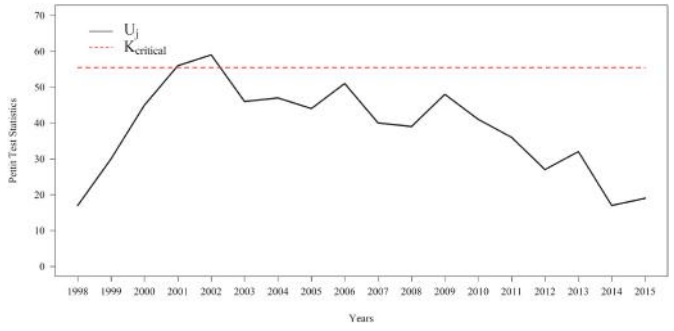

Fig. 6. Pettit test applied to the time series of fire foci of the state of Minas Gerais from 1998 to 2015.

the Northern Minas and Jequitinhonha mesoregions, due to the mainly agricultural areas with extensive plateaus, annual temperatures predominantly high and frequently observed water scarcity (Bastos and Gomes, 2010). The South/Southwest, Zona da Mata and Vale do Rio Doce mesoregions had a low record of fire foci, since they are predominantly agricultural regions with high altitudes, followed by well-distributed rainfall during the year. When compared to the first two mesoregions aforementioned, the Vale do Rio Doce has an irregular rainfall distribution and warm climate (Bastos and Gomes, 2010). The South/Southwest and Zona da Mata mesoregions, in addition to maintaining a low spot record, these fire foci remained close to the medium spot class.

Regarding foci density, the mesoregions of the state of MG that stood out were Triângulo Mineiro, Jequitinhonha, Norte de Minas, and Nordeste de Minas in the 2001/2002 cycle. The exception was South of Minas/Southwest of Minas only in 2002 (Table 4). It is important to highlight the significant annual increase of the North of Minas of 280% (20,677 foci km^{-2}). During the 2001/2002 cycle, in the Southeast region there was a significant decrease in rainfall producing meteorological systems (South Atlantic Convergence Zone - SACZ and Frontier Systems - FS) and an increase in rain inhibiting meteorological systems (Atmospheric Block - BA and Upper Tropospheric Cyclonic Vortex - UTCV) – (Climanálise, 2020), which in turn change the temperature distribution and wind regime (Reboita et al., 2010; Mendes et al., 2019) and thus contributed to a significant increase in fire foci.

Fig. 9 shows the quarterly Burned Area for 2001 and 2002 in the state

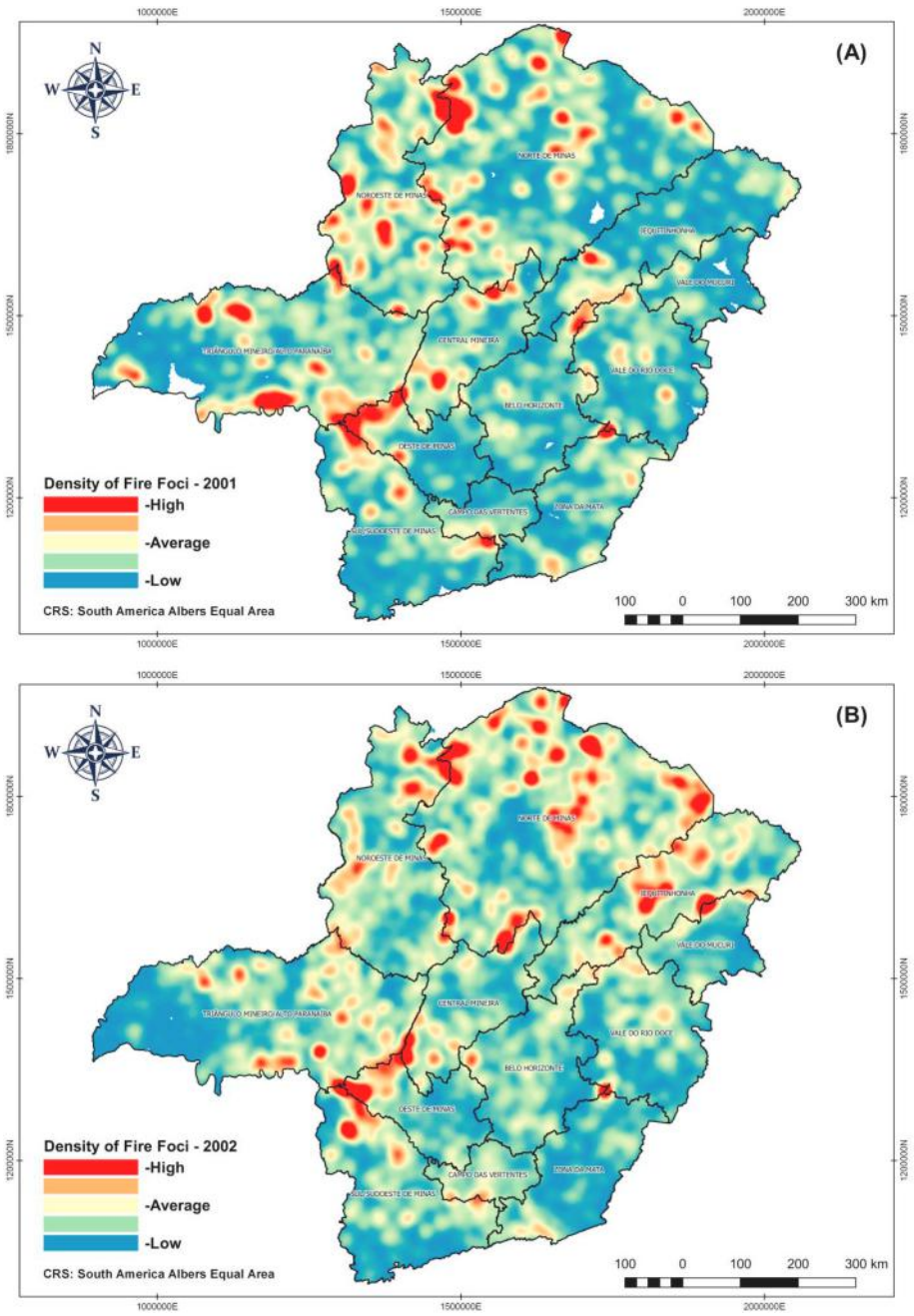

Fig. 7. Density map of annual fire foci for the mesoregions of Minas Gerais in 2001 (a) and 2002 (b).

of MG, where the years used were obtained from the sudden change in the time series of fire foci via Pettitt test (Fig. 6). In 2001, the main regions were North and Northwest MG, Triângulo Mineiro, Jequitinhonha, and South/Southwest of MG. In 2002, there was a significant increase in the Burned Area throughout the state of MG, especially in the North and Northwest mesoregions of MG and South/Southwest, highlighting the West mesoregion of MG. In all quarters, there was Burned Area in the state of MG, but the third quarter with 2,914.772 km^2 (2001) and 3,527.378 km^2 (2002) – increased 17% and fourth quarter with 373.598 km^2 (2001) and 3,039.226 km^2 (2002) – increased by 88%. Similar results were obtained by Carmona-Moreno et al. (2005) in the evaluation of burned areas on a global scale based on the quarterly evaluation and seasonal fire probability maps, the third and fourth quarters being highlighted for South America. The increases are also justified by the variability of rain producing and inhibiting meteorological systems in the Southeast region (Reboita et al., 2010; Caúla et al., 2015) and also for the changes in land use and land occupation via NDVI.

According to the average variability of NDVI for the state of MG (Fig. 10a), abundant vegetation (Table 5) is found in the central-eastern region of the state. This aspect of the vegetation is favored by the orography. Furthermore, there was a predominance of sparse vegetation in the Norte and Noroeste de Minas, Triangulo Mineiro, and Central Mineira. This pattern is due to land use and occupation, in this case by agricultural activities, such as sugarcane crops, mainly in the Triângulo Mineiro (Dias et al., 2018; Dias 2019).

The year 2001 (Fig. 10b), identified by the Pettit test (Fig. 6) and the Kernel density mapping (Figs. 7a, 8a and 8b), a positive NDVI anomaly (negative) was identified in the western (eastern) portion of the Triangulo Mineiro mesoregion. The Oeste de Minas mesoregion presented a negative NDVI anomaly (decrease in vegetative quality) associated with sugarcane crop, which in turn can trigger several fires and increased fire

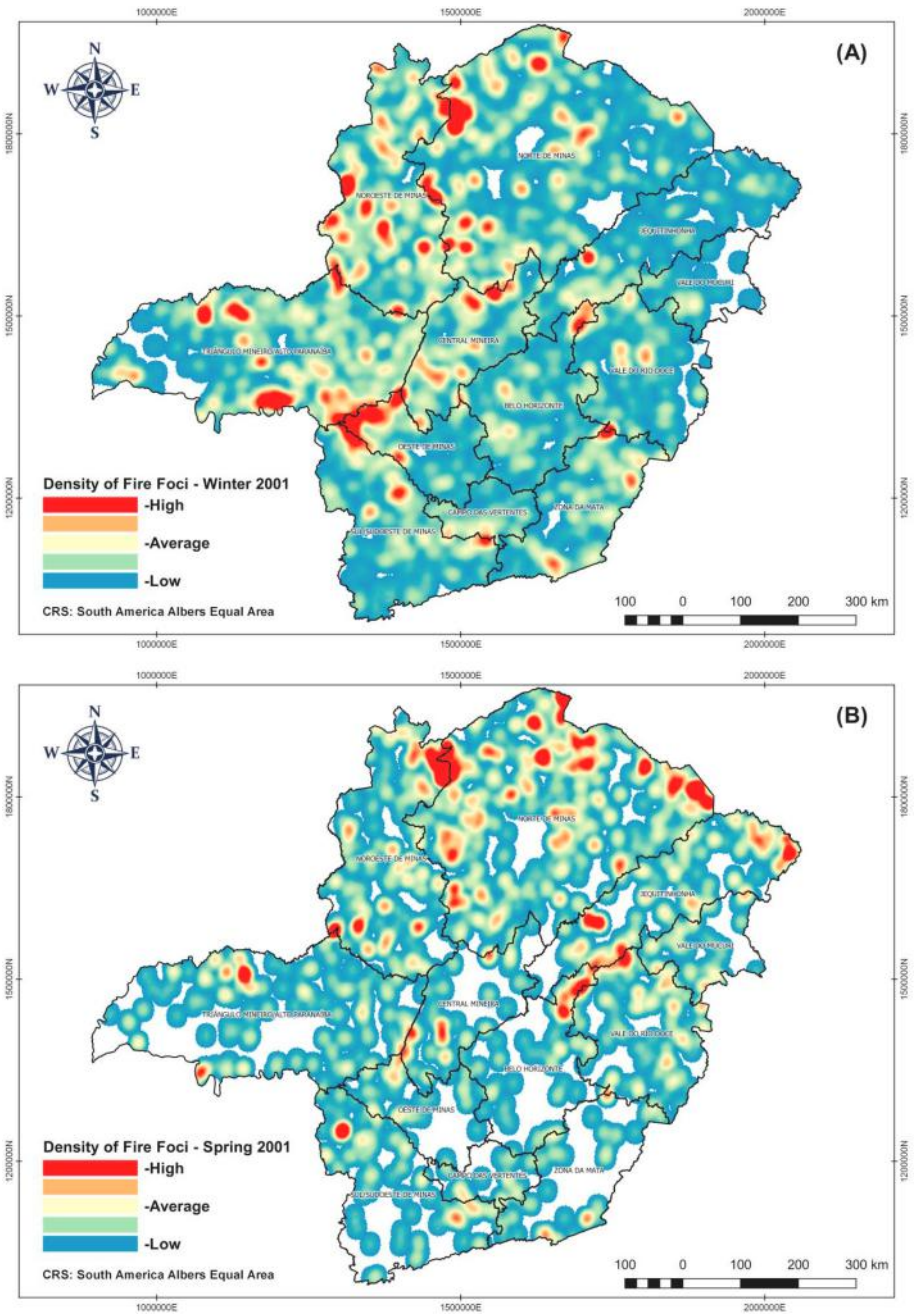

Fig. 8. Density map of monthly fire foci for the mesoregions of Minas Gerais in winter/2001 (A), spring/2001 (B), winter/2002 (C), and spring/2002 (D), respectively.

foci, as verified by the burned area in Fig. 9a, and verified by the results of Dias (2019). In 2002 (Fig. 10c), the anomalous pattern of NDVI was similar to 2001. However, in the 2001/2002 cycle, there was an occurrence of the ENSO phases, causing a change in the rainfall regime and an increase in the burned area (Fig. 9b).

Complementary to the fire foci mapping via Kernel density, the annual rainfall accumulated in 1998–2015 were evaluated (Fig. 11), where the high-density areas of fire foci are associated with negative anomalies, mainly in the Triângulo Mineiro mesoregions. Northwest and North of Minas (eastern sector), with a deficit between 75.0 and 225.0 mm. year^{-1}. The highest occurrence of fire foci in the Triângulo Mineiro is due to the sugarcane harvesting period, which occurs between April and November (Guimarães et al., 2010; Dos Reis and Brito, 2011). In spring and winter, we found that the mesoregions in the north of Minas Gerais (North and Northwest) had negative precipitation anomalies due to low rainfall and its irregular pattern (Reboita et al., 2015), with a deficit between −37.5 mm. year^{-1} and 150.0 mm. year^{-1}, which favored the increased fire foci records.

Regarding the relational pattern, there was a high magnitude positive linear correlation between the evaluated vegetation indices. These indices correlated negatively in high magnitude with LST and in low magnitude with fire foci. Highlight for positive correlation, but of low magnitude between LST and fire foci, followed by rainfall that correlated negatively and in low magnitude with LST and fire foci (Fig. 12). This technique was used by Oliveira-Júnior et al. (2020) to explain the relational pattern between rainfall and fire foci in State of Mato Grosso do Sul. Likewise, the authors observed a low magnitude negative correlation between these variables. These findings indicate that the

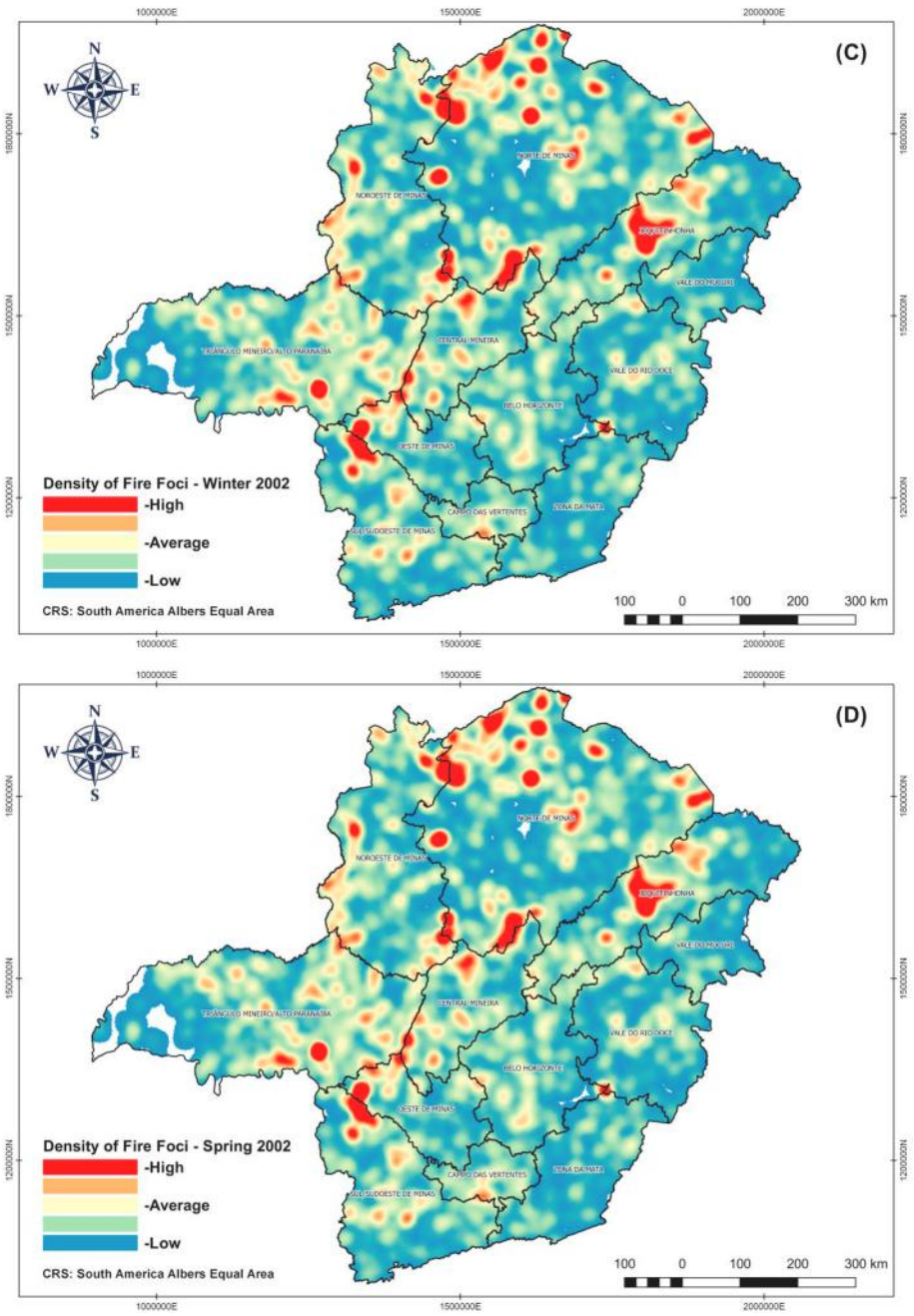

Fig. 8. (*continued*).

Table 4
Density of fire foci (foci. km^{-2}) in the mesoregions of the state of Minas Gerais for the years 2001 and 2002.

Mesorregions	2001 (foci. km^{-2})	2002 (foci. km^{-2})
Triângulo Mineiro	**3,857**	**9,817**
Noroeste de Minas	**3,545**	**8,515**
Norte de Minas	**5,435**	**20,677**
Jequitinhonha	**1,347**	**7,685**
Vale do Mucuri	0,415	2,072
Central Mineira	1,420	3,930
Metropolitana de Belo Horizonte	1,142	3,805
Vale do Rio Doce	1,205	3,897
Oeste de Minas	0,992	3,055
Campo das Vertentes	0,392	1,537
Sul de Minas/Sudoeste de Minas	1,632	**5,305**
Zona da Mata	1,137	2,477

occurrence of fire foci is not mainly influenced by rainfall, LST, in addition to the vegetation indices assessed (SAVI, NDVI, and EVI).

Oliveira-Júnior et al. (2020) relates fire foci obtained from BDQueimadas in Mato Grosso do Sul (MS) state for discussed the relationship between the fire foci and the phases of El Nino-South Oscillation (ENSO). However, there are marked differences between the studies and these are listed below: i) monthly rainfall data from 32 rainfall stations in the State of Mato Grosso do Sul were obtained from the Hidroweb - ANA platform and received statistical treatment of gap filling and data homogeneity (see Teodoro et al., 2015), unlike this study which uses the rainfall product CHIRPS already consolidated in the literature for evaluating rainfall anomalies; ii) we did not evaluate rainfall anomalies and only identified relational patterns between the three biomes (Mata Atlântica, Cerrado and Pantanal) existing in the state of Mato Grosso do Sul, the observed rainfall and the fire foci. This situation is the opposite of ours, where we do not evaluate the dynamics

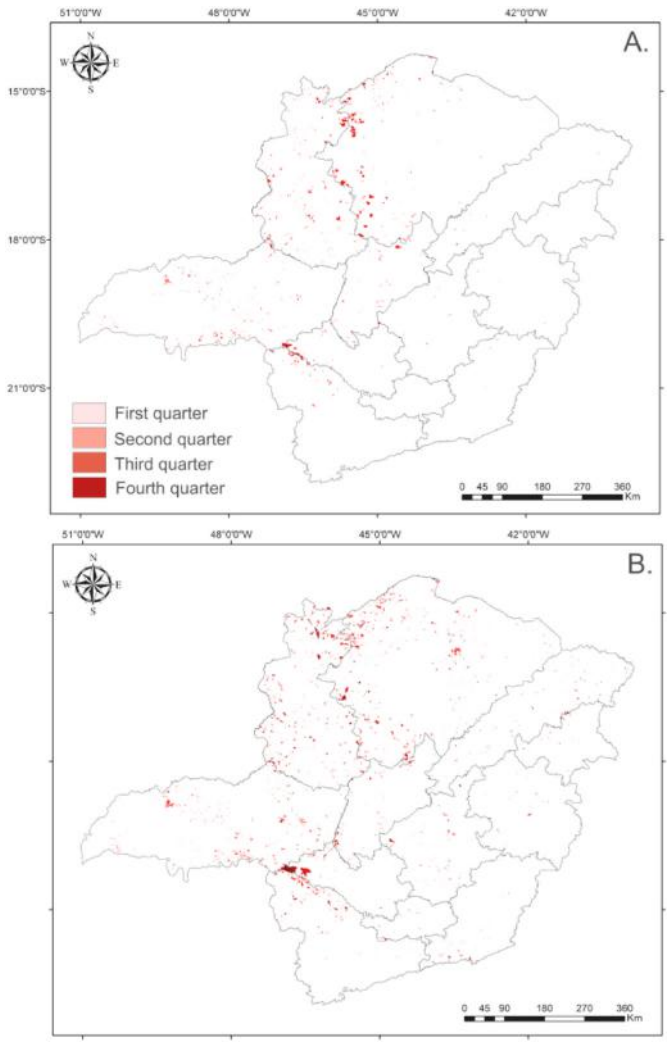

Fig. 9. Burned Area (km^2) obtained from the product MCD64A1.006 for the years 2001 (A) and 2002 (B) according to the Pettitt test.

of fire foci in the existing biomes of the state of Minas Gerais; iii) regarding multivariate analysis, the PCA was applied to the geographic, demographic and environmental data set and its interaction with fire foci, unlike the previous study which used another statistics; iv) another fact is that both states have totally different physiographic, climatological and environmental characteristics. For example, the MS state is in the Midwest region, where the meteorological systems are Upper Bolivia, Lower Chaco and Low-Level Jets, unlike the state of MG, where the meteorological systems are the Frontal Systems, South Atlantic Convergence Zone (SACZ), and Atmospheric Blocking (AB). Regarding the physiographic aspects, the state of MS has Cerrado, Atlantic Forest, and the Pantanal, the largest floodplain in the world. On the other hand, Minas Gerais has Cerrado, Atlantic Forest, and the Caatinga, the only essentially Brazilian biome, and also the mountain chains: Serras do Mar and Mantiqueira.

The result obtained from the KMO test regarding the quality of the data matrix was 0.75, categorized as good (Corrar et al., 2007). The lowest (highest) KMO value was verified by altitude (NDVI) with a value of 0.60 (0.95). After the KMO test, the optimal number of PCs to be selected from the Kaiser test was evaluated ($\lambda > 1$) (Kaiser 1960; Hongyu et al., 2016). The test indicated that three PCs, with a total of 71.49% of the explained variance. The assessment of the variability of geographical, demographic, meteorological variables, and vegetation proxies based on the year 2010 are found in Figs. 13 and 14 and in Table 6 and Table S1.

Fig. 13 illustrates the variability of Loadings from the three selected PCs, with a distinct pattern between them. The 1st PC resulted in 36.22% of the variance explained, with coefficients r between −0.71 (LST-D) and 0.93 (SAVI) (Table 6). The 1st PC showed that the highest positive (negative) values occurred in the variables: altitude, GPP, longitude, NDVI, Rainfall, and SAVI (Fire Foci, HDI-M, Latitude, LST-D and Population Density).

According to the spatial pattern of contribution of Loadings (Fig. 14a), negative (positive) values occurred in the North, West, and Center (South and East) regions of the state of MG. The mesoregions presenting negative contributions were Central Mineira, North of Minas, Northwest of Minas, West of Minas, Triangulo Mineiro and in the western part of the metropolitan mesoregion of Belo Horizonte (Fig. 1). There was a highlight for the latter, with the largest negative contribution (9.39). The positive contributions occurred in the extreme east and south of Minas Gerais, in the mesoregions of Campo das Vertentes, Jequitinhonha, South/Southwest Minas, Mucuri Valley, Rio Doce Valley, Zona da Mata and in the western part of the metropolitan mesoregion of Belo Horizonte. Highlight goes to the mesoregion of the Zona da Mata, which recorded the highest positive contribution (4.74), in the municipality of Alto Caparaó (ID 22).

It is important to highlight some associations related to this PC, such as the relevance of the variables extracted from vegetation indices (NDVI, SAVI, and GPP), which present a high positive correlation with fire foci. This is due to the characteristics of each biome belonging to the mesoregions. Regions with positive contributions are inserted in remaining areas of the Atlantic Forest that extends to the south and east of the State (Gonçalves et al., 2010). While negative contributions occurred in the Caatinga (in the north of the state), Campos Rupestres and Cerrado biomes in the central and western regions (Gonçalves et al., 2010).

According to Sano et al. (2008), 57% of the state of MG corresponds to the Cerrado Biome. However, 46% of the area is anthropic, located in the mesoregions of North Minas, Northwest Minas and Triangulo Mineiro. Part of these mesoregions were even transformed into pasture areas for agricultural cultivation, to which this characteristic influenced the value of the Loadings. Another highlight should be made to the variables LST-D and Fire Foci, both with negative correlations, the interaction in this contribution pattern corroborates the results found by Garcia et al. (2018) and Barros Santiago et al. (2019). In the case of LST-D, Garcia et al. (2018) found maximum temperature patterns with values between 25 and 35 °C in the North of Minas, Northwest of Minas, and Triângulo Mineiro. These high temperatures associated with undergrowth or degraded vegetation increase the plant stress, which favors the occurrence of fire foci, as verified by Bastos and Gomes (2010), Reis and Brito (2011), and Barros Santiago et al. (2019). Another interesting fact was the HDI-M variable in this PC, the lowest HDI-M values occurred in the North and Northwest mesoregions of Minas Gerais despite the rich plant biodiversity in the region (de Oliveira et al., 2015). As for the degree of contribution, the SAVI contributed 21.55% of the total variance relative to this PC, highlighting Belo Horizonte with 2.59% of the total variance.

The second PC resulted in 25.44% of the total variance explained, with a variation between −0.83 (Rainfall) and 0.89 (latitude). There is a change in the correlation pattern of the variables in this PC, among the negative ones are altitude, Rainfall, and HDI-M, while the positive ones would be latitude, longitude, and LST-D. The pattern of the second PC (Fig. 14b) showed significant change when compared with the first PC. The negative Loadings values occurred in the mesoregions located in the South of Minas Gerais: Triângulo Mineiro, South/Southwest of Minas and Southeast, Campo das Vertentes, Zona da Mata, and the southern part of the metropolitan mesoregion of Belo Horizonte, we again highlighted Belo Horizonte (ID 66) with the value of 4.24. While the positive values are found in the northern part of the mesoregions of North Minas, Northwest Minas, Jequitinhonha, Vale do Mucuri, Vale do Rio Doce, and

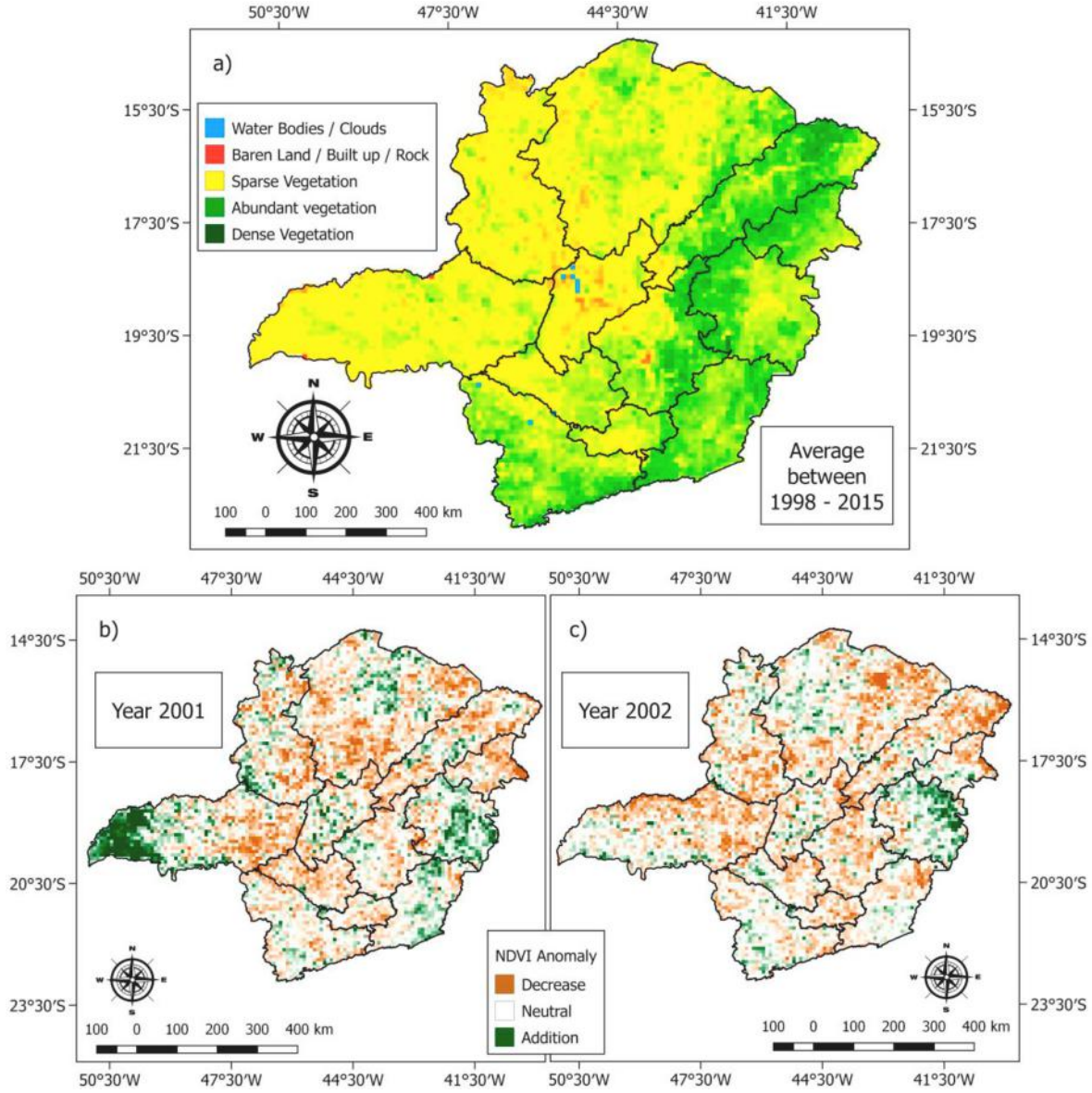

Fig. 10. NDVI médio (1998–2015) (a), NDVI anomaly - 2001 (b) and NDVI anomaly - 2002 (c).

Table 5
Categories and mean NDVI values between 1998 and 2015.

NDVI values	NDVI categories
−1.00 - 0.00	**Water Bodies/Clouds**
0.00–0.27	**Baren Land/Built up/Rock**
0.28–0.54	**Sparse Vegetation**
0.55–0.81	**Abundant vegetation**
0.81–1.00	**Dense Vegetation**

the northern part of the metropolitan mesoregion of Belo Horizonte. The highlight goes to the municipality of Jaguaraçú (ID 396) with a value of 4.60.

Regarding this PC, there was a change in the Loadings contribution sign, from negative to positive, when it moves in the northeast direction of Minas Gerais (North by Latitude and East by Longitude). Furthermore, such a pattern showed a possible association of the rainfall regime (due to the negative contributions of Altitude, Rainfall, and HDI-M) with orographic influence. This finding was similar to the results obtained by Souza et al. (2011), who by evaluating only the space-time rain pattern in the state of MG based on PCA and Cluster Analysis (CA), they detected the 1st PC exhibiting positive Loadings (negative) in the extreme south and east (central and northern region) of MG. However, despite the opposite sign, such changes are related to the number of variables used in this study, a total of 11, i.e., there will be influence of other variables in the outcome The mesoregions located in the South (Triângulo Mineiro, South/Southwest of Minas and Southeast, Campo das Vertentes, Zona da Mata) are located in areas above 650 m and are also influenced by FS and SACZ (Reboita et al., 2010). Meanwhile, the mesoregions of the northern part of the State (North of Minas and Northwest of Minas) are located in plains and slopes (between 300 and 600 m), and besides they have problems of regular rainfall, with values below 1,000 mm year^{-1} (Souza et al., 2015). Given the low rainfall in the region, it conditions the period of drought and thus increases the socioeconomic problems, possibly detected by the HDI-M (de Oliveira et al., 2015). Regarding the degree of contribution, the latitude contributed 28.35% of the total variance to this PC, while Belo Horizonte is again the most representative, with 0.75% of the total variance to this PC.

The third PC resulted in 9.82% of the total variance explained and the correlation coefficient ranged from −0.36 (Fire Foci) to 0.86

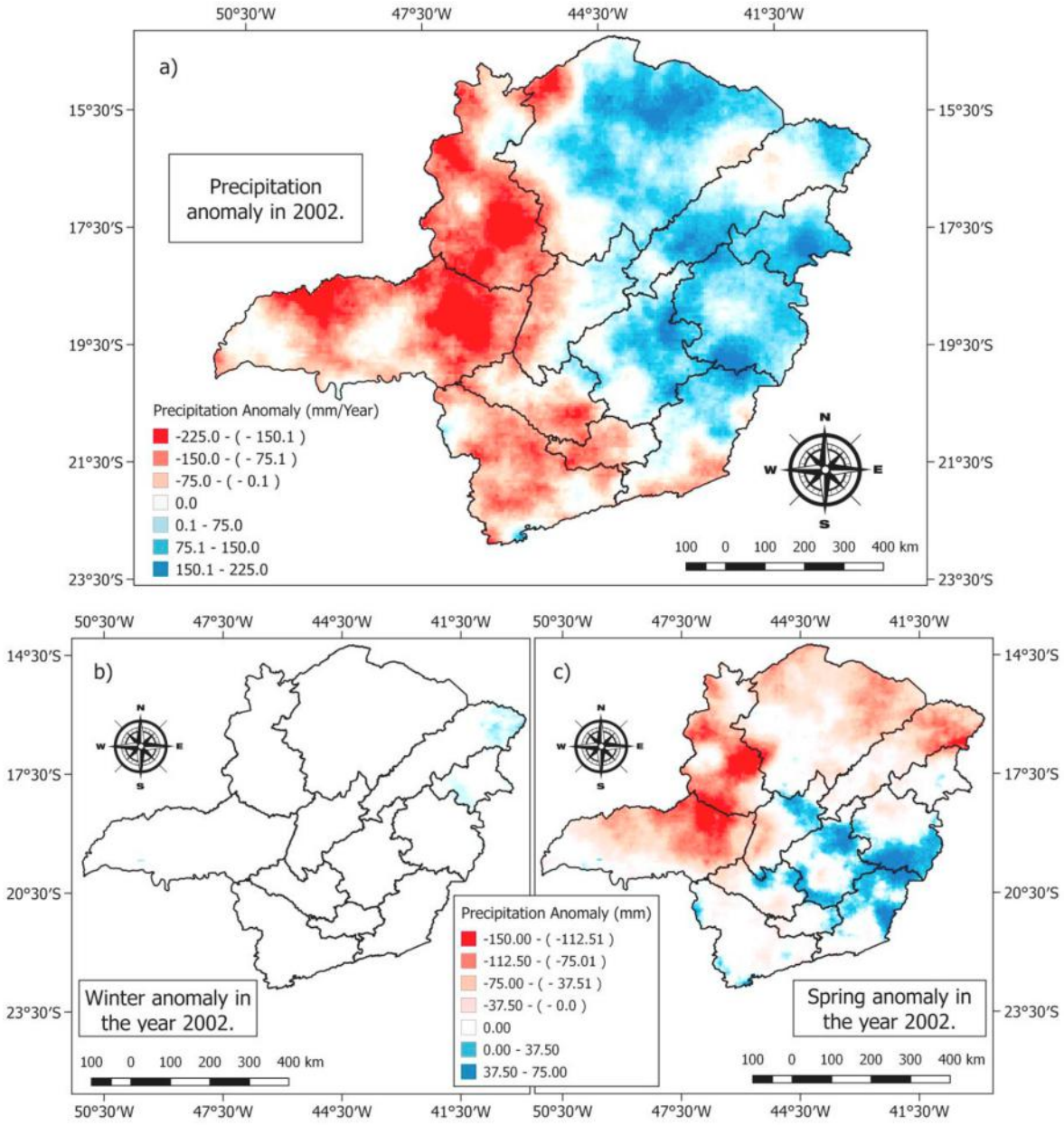

Fig. 11. Precipitation accumulated via CHIRPS product (in mm) for the mesoregions of the state of Minas Gerais: Anomaly in 2002 (a), Anomaly in 2002/winter (c) and Anomaly in 2002/spring (c).

(Populational Density). We verified that the correlation values were relatively low compared to previous PCs. Furthermore, the spatial variability of the Loadings' contribution (Fig. 14c) is different from the previous ones, where part of the Loadings ranged from −1 to 1. The significant contributions were the population density, especially in the metropolitan region of Belo Horizonte, which were positive, especially Belo Horizonte (ID 66), with a value of 20.40, while the municipality of Santos Dumont (ID 755) presented the highest negative contribution, with the value 3.19. Regarding the percentage of contribution, the variable Population Density represents 68.44% of the total variance of this PC, and again the municipality of Belo Horizonte is the most representative with 45.15% of the total variance explained.

4. Conclusions

The methodology developed in this study can be applied to the monitoring of forest fires in other states of Brazil and South American countries that are part of the BDQueimadas network, especially those with similar characteristics to the state of Minas Gerais. We highlight the use of several statistical tools, geotechnology, and remote sensing products in the construction of a theoretical-conceptual model applied in the environmental management of fire risk and fire foci dynamics based on free software (R and QGIS) and available data (fire foci, CHIRPS, and MODIS products) in an online format.

Based on statistical tests, the time series of fire foci in the state of Minas Gerais do not show normality and homogeneity of variances at 5% probability, which indicates that the time series does not follow a normal distribution. The descriptive and exploratory statistics used in the study point to August to October, with the highest occurrences of fire foci, months that deserve attention from environmental management. The Norte de Minas, Jequitinhonha, and Triângulo Mineiro regions stand out in the state regarding the dynamics of fire foci, mainly due to the accumulated totals, which together correspond to 58% of the fire foci in Minas Gerais.

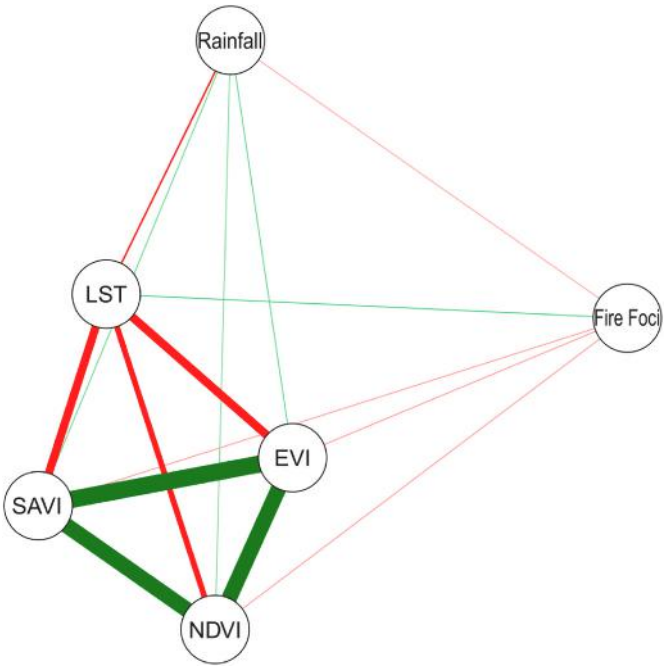

Fig. 12. Pearson's correlation network between the fire foci and the other variables (LST, Rainfall, SAVI, EVI, and NDVI) for the state of Minas Gerais.

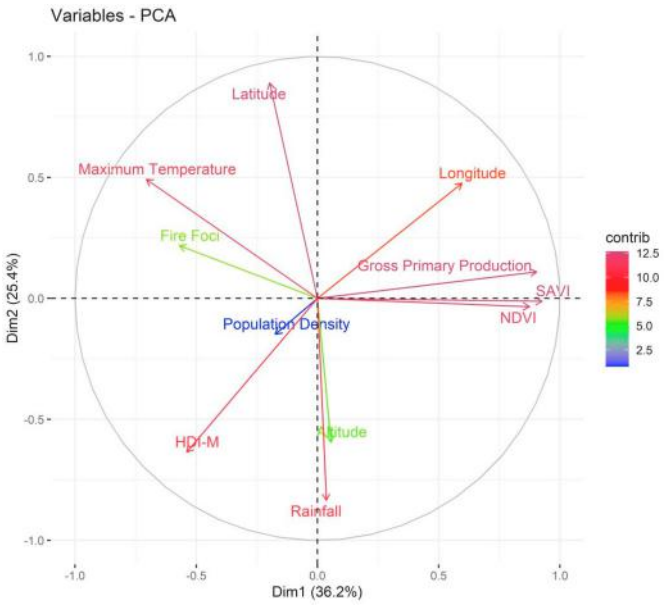

Fig. 13. Biplot of the degree of contribution of geographical, demographic, meteorological, and vegetation proxy variables from PC1, PC2, and PC3.

The Mann-Kendall test shows a significant trend in the increase of fire foci in the state, which shows that public policies to control forest fires and burnings deserve priority and urgency in the state. No less important is the mitigation of the consequences of fires, which require effective public policies to contain national deforestation, so that there is no dissociation between deforestation and fire foci. This occurs because burning is used as a practice for the initial cleaning and, when not controlled, it to give rise to fires. Burning also is used after deforestation to facilitate the entry of machines for use in extensive agriculture.

Pettitt's test indicates an abrupt change in the time series of fire foci from the 2001/2002 cycle (El Niño and La Niña moderated), which contributes to the annual increase and in winter and spring, which is

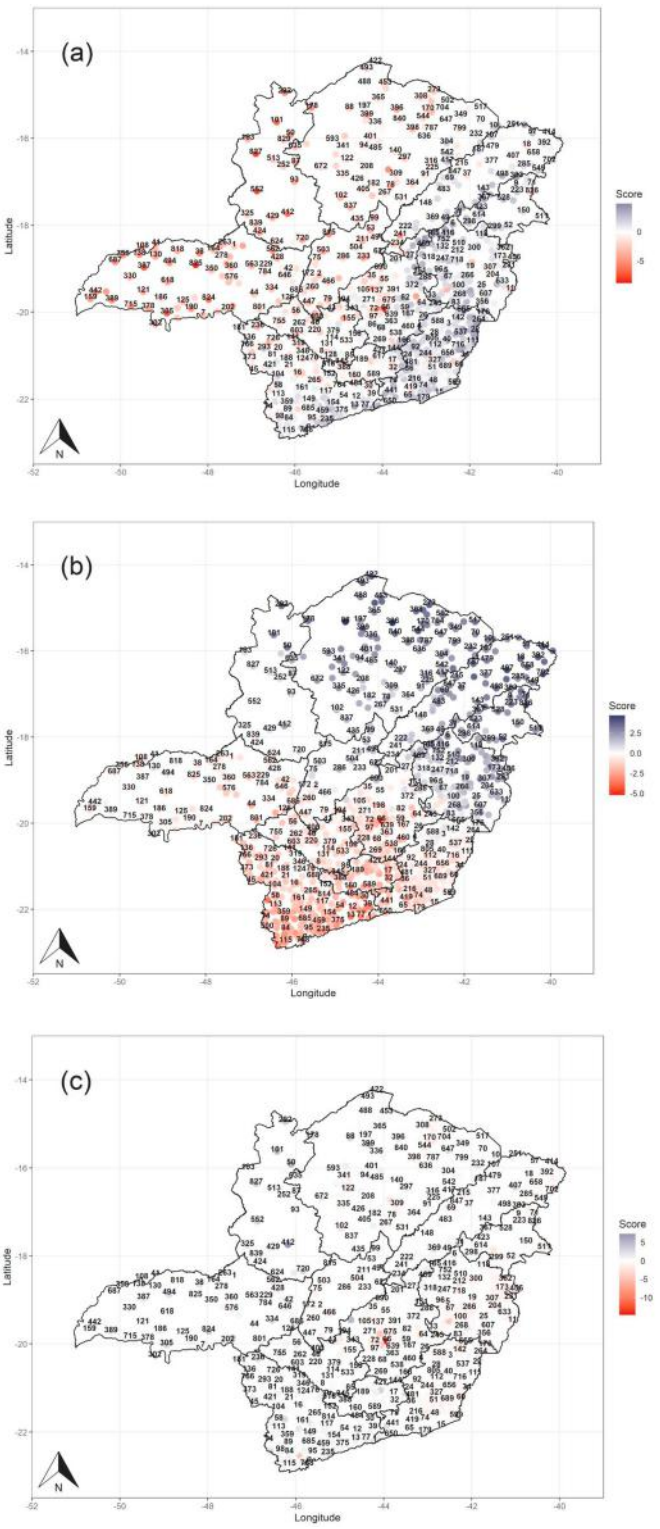

Fig. 14. Spatial distribution of PC Loadings in the state of Minas Gerais by Kaiser method,(a) 1ªPC, (b) 2ªPC, and (c) 3ªPC.

identified by Kernel density maps. The mapping of the fire foci indicates that the Norte and Jequitinhonha stand out from the other mesoregions regarding the density of the foci per area unit. The areas burned in the state of Minas Gerais via MODIS (MCD64A1) highlighted the Norte and Noroeste, Triângulo Mineiro, Jequitinhonha, and Sul/Sudoeste of MG. In 2001/2002 cycle, When used as base years for assessing CHIRPS product, the anomalies of winter and spring rainfall deserve attention

Table 6
Correlation Analysis (%) and Percentage Contribution (%) of each variable used in the principal component analysis extracted from the first three principal components (PC).

	Correlation (%)			Contributions for PC (%)		
Variables	PC1	PC2	PC3	PC1	PC2	PC3
Latitude	−0.20	0.89	−0.02	0.97	28.35	0.03
Longitude	0.60	0.48	0.35	8.92	8.09	11.25
Altitude	0.06	−0.59	−0.23	0.08	12.63	4.81
Fire Foci	−0.57	0.22	−0.36	8.15	1.70	11.87
Population Density	−0.17	−0.15	0.86	0.76	0.78	68.44
HDI-M	−0.54	−0.64	0.06	7.30	14.43	0.32
SAVI	0.93	−0.01	−0.13	21.55	0.01	1.47
NDVI	0.87	−0.03	−0.08	19.20	0.04	0.57
Rainfall	0.04	−0.83	0.00	0.03	24.90	0.00
LST-D	−0.71	0.49	−0.07	12.51	8.64	0.43
GPP	0.90	0.11	−0.09	20.52	0.43	0.81

from public managers, as there is a significant increase in fire foci due to the decrease in rainfall in Southeastern Brazil and the occurrence of dry air mass together with the variability of the meteorological systems contributing to prolonged droughts.

The PCA based on the three principal components results in 71.49% of the variation explained. Clearly, all PCs show a distinct pattern between them, especially on the spatial scale. Individually, the 1st PC is driven by variability in vegetation (GPP, NDVI, and SAVI) and temperature (LST-D). The 2 nd PC is influenced by rainfall associated with orography (altitude) in the northeastern direction of the state of MG, with direct influence on the HDI-M. The 3rd PC represents the population density pattern. The variables dependent on the three PCs are SAVI, Latitude, and Population Density. However, the SAVI is the most representative variable, with 11.12% of the total percentage, followed by Belo Horizonte as the most representative municipality in MG. The relational pattern between the environmental variable and vegetation indices shows that the Triângulo Mineiro mesoregion is related to the explanatory variable PRC, followed by Jequitinhonha with TMAX and Norte de Minas with NDVI and SAVI.

The limitations of our study were that the performance of environmental satellites was not evaluated, followed by the identification of the main meteorological systems contributing to the increased fire foci on the monthly scale in the state of Minas Gerais. As a suggestion for future studies, the influence of fire foci on existing biomes (Cerrado, Mata Atlântica and Caatinga) in the state of Minas Gerais and their relationship with ENSO phases, as well as the relational patterns between meteorological systems and fire risk over 20 years should be evaluated.

Credit author statement

A.A.R. Marinho, G. Gois, J.F. Oliveira-Júnior: Conceptualization, Methodology, and Calibration Data. W.L.F. Correia Filho, D.B. Santiago: Data curation, Writing – original draft. C.A. Silva Junior, P.E. Teodoro: Visualization, Investigation, and Calibration of Maps. P.E. Teodoro, A. Souza, G.F. Capristo-Silva: Statistic, Supervision, Validation. W.K. Freitas, J.P. Rogério: Validation, Writing- Reviewing and Editing.

Declaration of competing interest

The authors declare that they have no known competing financial interests or personal relationships that could have appeared to influence the work reported in this paper.

Acknowledgment

The authors are grateful to CPTEC/INPE for making fire foci data available through BDQueimadas, CLIMANÁLISE monthly climate bulletins, and to Climate Hazards Group (CHG) by data from CHIRPS. The second author thanks the Coordination for the Improvement of Higher-Level Personnel (CAPES) for granting the Post-Doctorate Scholarship (PNPD), together with the Graduate Program in Environmental Technology (PGTA). The third author thanks the National Council for Scientific and Technological Development (CNPq) for granting the level 2 Research Productivity Grant (309681/2019–7).

Appendix A. Supplementary data

Supplementary data to this article can be found online at https://doi.org/10.1016/j.jenvman.2020.111707.

References

Abatzoglou, J.T., Balch, J.K., Bradley, B.A., Kolden, C.A., 2018. Human-related ignitions concurrent with high winds promote large wildfires across the USA. Int. J. Wildland Fire 27, 377–386. https://doi.org/10.1071/WF17149.

Alhammadi, M.S., Glenn, E.P., 2008. Detecting date palm trees health and vegetation greenness change on the eastern coast of the United Arab Emirates using SAVI. Int. J. Rem. Sens. 29, 1745–1765. https://doi.org/10.1080/01431160701395195, 2008.

Althoff, T.D., Menezes, R.S.C., Carvalho, A.L., Pinto, A.S., Santiago, G.A.C.F., Ometo, J.P. H.B., Von Randow, C., Sampaio, E.V.S.B., 2016. Climate change impacts on the sustainability of the firewood harvest and vegetation and soil carbon stocks in a tropical dry forest in Santa Teresinha Municipality, Northeast Brazil. For. Ecol. Manag. 360, 367–375. https://doi.org/10.1016/j.foreco.2015.10.001.

Antunes, M.A.H., 2000. Uso de satélites para detecção de queimadas e para avaliação do risco de fogo. Ação Ambiental 12, 24–27.

Arantes Pereira, A., Alves Pereira, J.A., Morelli, F., Arantes Barros, D., 2012. Validação de focos de calor utilizados no monitoramento orbital de queimadas por meio de imagens. TM. Cerne 18, 335–343. https://doi.org/10.1590/S0104-77602012000200019.

Bai, L., Shi, C., Li, L., Yang, Y., Wu, J., 2018. Accuracy of CHIRPS satellite-rainfall products over mainland China. Rem. Sens. 10, 362. https://doi.org/10.3390/rs10030362.

Barros Santiago, D., Correia Filho, W.L.F., Oliveira-Júnior, J.F., Silva Junior, C.A., 2019. Mathematical modeling and use of orbital products in the environmental degradation of the Araripe Forest in the Brazilian Northeast. Modeling Earth Systems and Environment 1, 1–13. https://doi.org/10.1007/s40808-019-00614-x.

Bartlett, M.S., 1937. Properties of sufficiency and statistical tests. Proc. Roy. Soc. Lond. Math. Phys. Sci. 160, 268–282.

Bastos, S., Gomes, J.E., 2010. Dinâmica da agricultura no Estado de Minas Gerais: análise diferencial-estrutural para o período 1994 a 2008. Cedeplar. Universidade Federal de Minas Gerais.

Batista, A.C., 2004. Detecção de incêndios florestais por satélites. Floresta 34, 1–9. https://doi.org/10.5380/rf.v34i2.2402.

Bento-Gonçalves, A., Vieira, A., 2020. Wildfires in the wildland-urban interface: key concepts and evaluation methodologies. Sci. Total Environ. 707, 135592. https://doi.org/10.1016/j.scitotenv.2019.135592.

Boer, M.M., Resco de Dios, V., Bradstock, R.A., 2020. Unprecedented burn area of Australian mega forest fires. Nat. Clim. Change 10, 171–172. https://doi.org/10.1038/s41558-020-0716-1.

Boschetti, L., Roy, D., Barbosa, P., Boca, R., Justice, C., 2008. A MODIS assessment of the summer 2007 extent burned in Greece. Int. J. Rem. Sens. 29, 2433–2436. https://doi.org/10.1080/01431160701874561.

Brando, P.M., Paolucci, Lucas, Ummenhofer, C.C., Ordway, E.M., Hartmann, H., Cattau, M.E., Rattis, L., Medjibe, V., Coe, M.T., Balch, J., 2019. Droughts, wildfires, and forest carbon cycling: a pantropical synthesis. Annu. Rev. Earth Planet Sci. 47, 555–581. https://doi.org/10.1146/annurev-earth-082517-010235.

Camargos, V.L., Ribeiro, G.A., Da Silva, A.F., Martins, S.V., Da Silva Carmo, F.M., 2015. Estudo do comportamento do fogo em um trecho de floresta estacional semidecídua no município de Viçosa, Minas Gerais. Ciência Florest. 25, 537–545. https://doi.org/10.5902/1980509819605.

Carmona-Moreno, C., Belward, A., Malingreau, J.P., Hartley, A., Garcia-Alegre, M., Antonovisk, M., Buchshtaber, V., Pivovarov, V., 2005. Characterizing interannual variations in global fire calendar using data from Earth observing satellites. Global Change Biol. 11, 1537–1555. https://doi.org/10.1111/j.1365-2486.2005.001003.x.

Castro, H.A., Gonçalves, K.S., Hacon, S.S., 2009. Trend of mortality from respiratory disease in elderly and the forest fires in the state of Rondônia/Brazil: period between 1998 and 2005. Ciência Saúde Coletiva 14, 2083–2090.

Caúla, R.H., Oliveira-Júnior, J.F., Lyra, G.B., Delgado, R.C., Heilbron Filho, P.F.L., 2015. Overview of fire foci causes and locations in Brazil based on meteorological satellite data from 1998 to 2011. Environmental Earth Sciences (Print) 74, 1497–1508. https://doi.org/10.1007/s12665-015-4142-z.

Caúla, R.H., Oliveira-Júnior, J.F., Gois, G., Delgado, R.C., Pimentel, L.C.G., Teodoro, P. E., 2016. Non-parametric statistics applied to fire foci obtained by meteorological satellites and their relationship to the MCD12Q1 product in the state of Rio de Janeiro, Southeast - Brazil. Land Degrad. Dev. 28, 1056–1067. https://doi.org/10.1002/ldr.2574.

Chuvieco, E., Mouilot, F., Van der Werf, G.R., Miguel, J.S., Tanase, M., Koutsias, N., García, M., Yebra, M., Padilla, M., Gitas, I., Heil, A., Hawbaker, T.J., Giglio, L., 2019. Historical background and current developments for mapping burned area from

satellite Earth observation. Rem. Sens. Environ. 225, 45–64. https://doi.org/10.1016/j.rse.2019.02.013.
Clemente, S.S., Oliveira Júnior, J.F., Louzada, M.A.P., 2017. Focos de Calor na Mata Atlântica do estado do Rio de Janeiro. Revista Brasileira de Meteorologia 32, 1–9. https://doi.org/10.1590/0102-7786324014.
Climanálise - CPTEC/INPE. Boletins Mensais Climatológicos. http://climanalise.cptec.inpe.br/~rclimanl/boletim/: Acesso em 23 de maio de 2020.
Corrar, L.J., Paulo, E., Dias Filho, J.M., 2007. Análise Multivariada - para os Cursos de Administração, Ciências Contábeis e Economia. In: Atlas, São Paulo, 1ª Ed., p. 344.
Coutinho, L.M., 1990. Fire in the ecology of the Brazilian cerrado. In: Goldammer, J.G. (Ed.), Fire in the Tropical Biota, vol. 6. Springer-Verlag, New York, pp. 82–105 cap.
CPTEC - Centro de Previsão do Tempo e Estudos Climáticos, 2018. BDQueimadas. http://pirandira.cptec.inpe.br/queimadas/. (Accessed 14 February 2018).
Crutzen, P.J., Andrea, M.O., 1990. Biomes burning in the tropics: impact on atmospheric chemistry and biogeochemical cycles. Science 250, 1669–1679. https://doi.org/10.1126/science.250.4988.1669.
de Oliveira, D.A., de Abreu Moreira, P., de Melo Júnior, A.F., Pimenta, M.A.S., 2015. Potential da biodiversidade vegetal da Região Norte do Estado de Minas Gerais. Unimontes Científica 8 (1), 23–34.
Dean, W., Ferro, A., 1996. Fogo: a história e a devastação da Mata Atlântica. São Paulo, Companhia das Letras, p. 23.
Dias, B.A.S., Schultz, B., Sanches, I.D.A., Eberhardt, I.D., dos Santos Rosendo, J., 2018. Identificação do modo de colheita da cana-de-açúcar em imagens multitemporais landsat-like. Rev. Bras. Cartogr. 70 (2), 527–554.
Dias, B.A.S., 2019. Mapeamento da cana-de-açúcar em Minas Gerais. 112 f. Dissertação (Mestrado em Geografia) - universidade Federal de Uberlândia, Uberlândia. Disponível em. https://doi.org/10.14393/ufu.di.2019.615.
Didan, K., 2015. MYD13C2 MODIS/Aqua Vegetation Indices Monthly L3 Global 0.05Deg CMG V006 [Data Set]. NASA EOSDIS Land Processes DAAC. https://doi.org/10.5067/MODIS/MYD13C2.006. Accessed 2019-08-19 from.
Diniz, C.G., Souza, A.A.A., Santos, D.C., Dias, M.C., Luz, N.C., Moraes, D.R.V., Maia, J.S., Gomes, A.R., Narvaes, I.S., Valeriano, D.M., Maurano, L.E.P., Adami, M., 2015. DETER-B: the new Amazon near real-time deforestation detection system. Journal of Selected Topics in Applied Earth Observations and Remote Sensing 8, 3619–3628. https://doi.org/10.1109/JSTARS.2015.2437075.
Donaldson, K., Stonea, V., Clouter, A., Renwick, L., MacNee, W., 2001. Ultrafine particles. Occup. Environ. Med. 58, 211–216. https://doi.org/10.1136/oem.58.3.211.
Donaldson, K., Stonea, V., Gilmour, P.S., BrownDM, MacNee, W., 2000. Ultrafine particles: mechanisms of lung injury. Phil. Trans. Math. Phys. Eng. Sci. 358, 2741–2749. https://doi.org/10.1098/rsta.2000.0681.
Dozier, J., 1981. A method for satellite identification of surface temperature fields of subpixel resolution. Rem. Sens. Environ. 11, 221–229.
Duan, Z., Liu, J., Tuo, Y., Chiogna, G., Disse, M., 2016. Evaluation of eight high spatial resolution gridded precipitation products in Adige Basin (Italy) at multiple temporal and spatial scales. Sci. Total Environ. 573, 1536–1553. https://doi.org/10.1016/j.scitotenv.2016.08.213.
Fernandes, M.F., Queiroz, L.P., 2018. Vegetação e flora da Caatinga. Ciencia e Cult. 70 (4), 51–56. https://doi.org/10.21800/2317-66602018000400014.
Fiedler, N.C., Fiedler, N.C., Rezende, A.V., Venturoili, F., 2004. Efeito de incêndios florestais na estrutura e composição florística de uma área de cerrado sensu stricto na fazenda Água Limpa-DF. Rev. Árvore 28, 129–138. https://doi.org/10.1590/S0100-67622004000100017.
Fiedler, N.C., Merlo, D.A., Medeiros, M.B., 2006. Ocorrência de incêndios florestais no Parque Nacional da Chapada dos Veadeiros, Goiás. Ciência Florest. 16, 153–161. https://doi.org/10.5902/198050981896.
Freitas, W.K., Gois, G., Pereira Junior, E.R., Oliveira-Júnior, J.F., Magalhães, L.M.S., Brasil, F.C., Sobral, B.S., 2020. Influence of fire foci on forest cover in the Atlantic Forest of Rio de Janeiro, Brazil. Ecol. Indicat. 115, 1–10. https://doi.org/10.1016/j.ecolind.2020.106340.
FUNDAÇÃO SOS MATA ATLÂNTICA, INPE, 2002. Atlas dos remanescentes florestais da Mata Atlântica e ecossistemas associados no período de 1995-2000. Relatório final, São Paulo.
Funk, C., Peterson, P., Landsfeld, M., Pedreros, D., Verdin, J., Shukla, S., Husak, G., Rowland, J., Harrison, L., Hoell, A., Michaelsen, J., 2015a. The climate hazards infrared precipitation with record for monitoring extremes. Scientific Data 2 (1), 10–66. https://doi.org/10.1038/sdata.2015.66.
Funk, C., Verdin, A., Michaelsen, J., Peterson, P., Pedreros, D., Husak, G.A., 2015b. Global satellite-assisted precipitation climatology. Earth Syst. Sci. Data 7, 275–287. https://doi.org/10.5194/essd-7-275-2015b.
Garcia, S.R., dos Santos, D.F., Martins, F.B., Torres, R.R., 2018. Aspectos climatológicos associados ao cultivo da oliveira (Olea europaea L.) em Minas Gerais. Revista Brasileira de Climatologia 22. https://doi.org/10.5380/abclima.v22i0.56825.
Ghazoul, J., Burivalova, Z., Garcia-Ulloa, J., King, L.A., 2015. Conceptualizing forest degradation. Trends Ecol. Evol. 30, 622–632. https://doi.org/10.1016/j.tree.2015.08.001.
Giglio, L., Descloitres, J., Justice, C.O., Kaufman, Y., 2003. An enhanced contextual fire detection algorithm for MODIS. Rem. Sens. Environ. 87, 273–282.
Gois, G., Freitas, W.K., Oliveira, Júnior, JF, 2020. Spatial-temporal of fire foci in the state of Rio de Janeiro, Brazil. Biosci. J. 36, 1008–1017. https://doi.org/10.14393/BJ-v36n3a2020-47769.
Gualberto, J.A., 2020. Comparação das técnicas Kernel e Krigagem indicativa na predição de valores de variáveis espacialmente distribuídas-estudos de caso. Dissertação de Mestrado – UNESP, p. 33.
Guimarães, D.P., dos Reis, R.J., Landau, E.C., 2010. Índices pluviométricos em Minas Gerais. Embrapa Milho e Sorgo-Boletim de Pesquisa e Desenvolvimento (INFOTECA-E).
Hongyu, K., Sandanielo, V.L.M., de Oliveira Junior, G.J., 2016. Análise de componentes principais: resumo teórico, aplicação e interpretação. E&S Engineering and Science 5 (1), 83–90. https://doi.org/10.18607/ES201653398.
Huete, A., Didan, K., Miura, T., Rodriguez, E.P., Gao, X., Ferreira, L.G., 2002. Overview of the radiometric and biophysical performance of the MODIS vegetation indices. Rem. Sens. Environ. 83, 195–213. https://doi.org/10.1016/S0034-4257(02)00096-2.
Ibf - Instituto Brasileiro de Florestas, 2019. Bioma Mata Atlântica. Acesso em 28 de janeiro de. https://www.ibflorestas.org.br/bioma-mata-atlantica.html.
Ibge - Instituto Brasileiro de Geografia e Estatística. Geociências. Disponível em: <http://www.ibge.gov.br/home/geociencias/areaterritorial/principal.shtm>. Acesso em 21/09/2017.
IEFMG - Instituto Estadual de Florestas de Minas Gerais, 2019. A cobertura vegetal de Minas Gerais. Disponível em. Acesso em 28 de janeiro de. http://www.ief.mg.gov.br/florestas.
INPE – Instituto Nacional de Pesquisas Espaciais. Disponível em. http://www.inpe.br/noticias/noticia.php?Cod_Noticia=5138>. Acesso em 10 de setembro de 2019.
Kaiser, H.F., 1960. The application of electronic computers to factor analysis. Psychol. Meas. 20, 141–151.
Kassomenos, P., Paschalidou, A.K., 2017. Studying the synoptic wildfire climatology in Greece. Implications to wildfire management. In: Perspectives on Atmospheric Sciences. Springer, Cham, pp. 733–739. https://doi.org/10.1007/978-3-319-35095-0_105.
Katsanos, D., Retalis, A., Michaelides, S., 2016. Validation of a high-resolution precipitation database (CHIRPS) over Cyprus for a 30-year period. Atmos. Res. 169, 459–464. https://doi.org/10.1016/j.atmosres.2015.05.015.
Kelly, L., Brotons, L., 2017. Using fire to promote biodiversity. Science 355, 1264–1265. https://doi.org/10.1126/science.aam7672.
Kodandapani, N., Parks, S.A., 2019. Effects of drought on wildfires in forest landscapes of the Western Ghats, India. Int. J. Wildland Fire 28 (6), 431–444. https://doi.org/10.1071/WF18188.
Koutsias, N., Martínez-Fernández, J., Allgöwer, B., 2010. Do factors causing wildfires vary in space? Evidence from geographically weighted regression. GIScience Remote Sens. 47, 221–240. https://doi.org/10.2747/1548-1603.47.2.221.
Lima, G.S., 2000. A prevenção de incêndios florestais no estado de Minas Gerais. Floresta 30, 37–43. https://doi.org/10.5380/rf.v30i12.2364.
Lima, M., Vale, J.C.E., Costa, G.M., Santos, R.C., Correia, Filho, Wlf, Gois, G., Oliveira Júnior, J.F., Teodoro, P.E., Rossi, F.S., Silva Junior, Ca, 2020. The forests in the indigenous lands in Brazil in peril. Land Use Pol. 90, 1–3. https://doi.org/10.1016/j.landusepol.2019.104258.
Matson, M., Dozier, J., 1981. Identification of subresolution high temperature sources using a thermal IR sensor. Photogramm. Eng. Rem. Sens. 47, 1311–1318.
MCTI, 2016. Terceira Comunicação Nacional do Brasil à Convenção-Quadro das Nações Unidas sobre Mudança do Clima – Sumário Executivo, 45p/Ministério da Ciência, Tecnologia e Inovação, Brasília, ISBN 978-85-88063-18-1.
Medeiros, J.S., Câmara, G., 1996. Geoprocessamento para projetos ambientais. INPE.
Meira, M.R., Cabacinha, C.D., 2016. Manejo sustentável do barbatimão no Norte de Minas Gerais. Floresta Ambiente 23, 61–69. https://doi.org/10.1590/2179-8087.041213.
Meira-Neto, J.A.A., Martins, F.R., Souza, A.L., 2005. Influência da cobertura e do solo na composição florística do sub-bosque em uma floresta estacional semidecidual em Viçosa, MG, Brasil. Acta Bot. Bras. 19, 473–486. https://doi.org/10.1590/S0102-33062005000300007.
Mendes, M.C.D., Aragão, M.R.S., Correia, M.F., 2019. Bloqueios Atmosféricos sobre os Oceanos Pacífico Sudeste e Atlântico Sul: Características Sinótico-Dinâmicas e Termodinâmicas, vol. 42. Anuário do Instituto de Geociências – UFRJ, pp. 309–324. https://doi.org/10.11137/2019_2_309_324.
Minuzzi, R.B., Sediyama, G.C., Barbosa, E.M., Junior, Melo, Jcf, 2007. Climatologia do comportamento do período chuvoso da região sudeste do Brasil. Revista Brasileira de Meteorologia 22, 338–344. https://doi.org/10.1590/S0102-77862007000300007.
Mittermeier, R.A., Gil, R.P., Hoffman, M., Pilgrim, J., Brooks, T., Mittermeier, C.G., Lamoreux, J., Fonseca, G.A.B., 2005. Hotfire Foci Revisited: Earth's Biologically Richest and Most Endangered Terrestrial Ecoregions. 2ªed. University of Chicago Press, Boston.
MMA – Ministério do Meio Ambiente. Plano de Ação para Prevenção e Controle do Desmatamento na Amazônia Legal (PPCDAm). Disponível em: https://www.mma.gov.br/informma/item/616-preven%C3%A7%C3%A3o-e-controle-do-desmatamento-na-amaz%C3%B4nia>. Acesso em 10 de setembro de 2019.
Moreno, M.V., Conedera, M., Chuvieco, E., Pezzatti, G.B., 2014. Fire regime changes and major driving forces in Spain from 1968 to 2010. Environ. Sci. Pol. 37, 11–22. https://doi.org/10.1016/j.envsci.2013.08.005.
Musinsky, J., Tabor, K., Cano, C.A., Ledezma, J.C., Mendoza, E., Andriambolantsoa, R., Sajudin, E.R., 2018. Conservation impacts of a near real--time forest monitoring and alert system for the tropics. Remote Sensing in Ecology and Conservation 4, 189–196. https://doi.org/10.1002/rse2.78.
Nunes, M.T.O., Sousa, G.M., Tomzhinski, G.W., Oliveira-Júnior, J.F., Fernandes, M.C., 2015. Factors influencing on susceptibility Forestry fire in itatiaia national park. Anu. do Inst. Geociencias 38, 54–62. https://doi.org/10.11137/2015_1_54_62.
Oliveira, U.C., De Oliveira, O.S., 2017. Mapas de Kernel como Subsídio à Gestão Ambiental: análise dos Focos de Calor na Bacia Hidrográfica do Rio Acaraú, Ceará, nos Anos 2010 a 2015. Espaço Aberto 7, 87–99.

Oliveira-Júnior, J.F., Sousa, G.M., Nunes, M.T.O., Fernandes, M.C., Tomzhinski, G.W., 2017. Relationshipbetween SPI and ROI in itatiaia national park. Floresta e Ambiente 24, e20160031. https://doi.org/10.1590/2179-8087.003116.

Oliveira-Júnior, J.F., Teodoro, P.E., Silva Junior, C.A., Baio, F.H.R., Gava, R., Capristo-Silva, G.F., Gois, G., Correia Filho, W.L.F., Lima, M.G., Santiago, D.B., Freitas, W.K., Santos, P.J., Costa, M., 2020. Fire foci related to rainfall and biomes of the state of Mato Grosso do Sul, Brazil. Agric. For. Meteorol. 282, 1–13. https://doi.org/10.1016/j.agrformet.2019.107861.

Paredes-Trejo, F.J., Barbosa, H.A., Lakshmi Kumar, T.V., 2017. Validating CHIRPS-based satellite precipitation estimates in Northeast Brazil. J. Arid Environ. 26–40. https://doi.org/10.1016/j.jaridenv.2016.12.009.

Pausas, J.G., Keeley, J.E., 2019. Wildfires as an ecosystem service. Front. Ecol. Environ. 17, 289–295. https://doi.org/10.1002/fee.2044.

Pettit, A.N., 1979. A non-parametric approach to the change-point problem. Applied Statistics 28, 126–135. https://www.jstor.org/stable/2346729.

PPCDAm, 2016b. Plano de Ação para Prevenção e Controle do Desmatamento na Amazônia Legal – Documento Base: Contexto e Análises dos Dados. Ministério do Meio Ambiente. URL: https://www.mma.gov.br/informma/item/616-prevenção-e-controle-do-desmatamento-na-amazônia/(2016a) PPCDAm - Plano de Ação para Prevenção e Controle do Desmatamento na Amazônia Legal – Plano Operativo 2016-2020: Objetivos e Linhas de Ação. MMA. URL: https://www.mma.gov.br/informma/item/616-prevenção-e-controle-do-desmatamento-na-amazônia/.

Prakash, S., 2019. Performance assessment of CHIRPS, MSWEP, SM2RAIN-CCI, and TMPA precipitation products across India. J. Hydrol. 571, 59. https://doi.org/10.1016/j.jhydrol.2019.01.036.

Preisendorfer, R.W., 1988. Principal component analysis. In: Meteorology and Oceanography. Elsevier, New York.

QGIS Development Team, 2009. Quantum Geographic Information System Version 2.14. Open Source Geospatial Foundation. http://qgis.osgeo.org.

R Development Core TeamR, 2011. A Language and Environment for Statistical Computing. R Foundation for Statistical Computing, Vienna, Austria, ISBN 3-900051-07-0. http://www.R-project.org/.

Reboita, M.S., Gan, M.A., Rocha, R.P., Ambrizzi, T., 2010. Regimes de precipitação na América do Sul: uma revisão bibliográfica. Revista Brasileira de Meteorologia 25, 185–204. https://doi.org/10.1590/S0102-77862010000200004.

Reboita, M.S., Rodrigues, M., Silva, L.F., Alves, M.A., 2015. Aspectos climáticos do estado de Minas Gerais. Revista Brasileira de Climatologia 17, 206–226. https://doi.org/10.5380/abclima.v17i0.41493.

Reis, L.N.G., Brito, J.L.S., 2011. Mapeamento da cana-de-açúcar na mesorregião do Triângulo Mineiro/Alto Paranaíba-MG (2008/2009;2010/2011). Revista Tamoios 7, 37–47. https://doi.org/10.12957/tamoios.2011.4571.

Ribeiro, M.C., Figueira, J.E.C., 2011. Uma abordagem histórica do fogo no Parque Nacional da Serra do Cipó, Minas Gerais–Brasil. Biodiversidade Brasileira 2, 212–227.

Viewed 29 may 2020] Rouse, J., Haas, R., Schell, J., Deering, D., Harlan, J., 1974. Monitoring the Vernal Advancement of Retrogradation of Natural Vegetation. Final Report [online]. Greenbelt: NASA/GSFC, 371 pp. Available from:http://ntrs.nasa.gov/archive/nasa/casi.ntrs.nasa.gov/19740008955.pdf.

Running, S.W., 2006. Is global warming causing more, larger wildfires? Science 313, 927–928. https://doi.org/10.1126/science.1130370.

Running, S.W., Zhao, M., 2015. Daily GPP and annual NPP (MOD17A2/A3) products NASA earth observing system MODIS land algorithm.

Sano, Edson, Eyji Rosa, Roberto, Brito, Luís Silva, Jorge, Ferreira, Laerte, Guimarães, 2008. Mapeamento semidetalhado do uso da terra do Bioma Cerrado. Pesqui. Agropecuária Bras. 43 (1), 153–156. https://doi.org/10.1590/S0100-204X2008000100020.

Sayad, Y.O., Mousannif, H., Moatassime, H.A., 2019. Predictive modeling of wildfires: a new dataset and machine learning approach. Fire Saf. J. 104, 130–146. https://doi.org/10.1016/j.firesaf.2019.01.006.

Schoennagel, T., Veblen, T.T., Romme, W.H., 2004. The interaction of fire, fuels, and climate across Rocky Mountain Forests. Bioscience 54, 661–676. https://doi.org/10.1641/0006-3568(2004)054[0661:TIOFFA]2.0.CO;2.

Setzer, A.W., Sismanoglu, R.A., 2018. Risco de Fogo – resumo do método de Cálculo (versão 5 – fevereiro - 2006). Disponível em. Acesso em: 20 de outubro de. http://pirandira.cptec.inpe.br/queimadas/doc_RF_2007.pdf.

Setzer, A.W., Verstraete, M.M., 1994. Fire and glint in AVHRR's channel 3: a possible reason for the non-saturation mystery. Int. J. Rem. Sens. 15, 711–718. https://doi.org/10.1080/01431169408954111.

Shapiro, S.S., Wilk, M.B., 1965. An analysis of variance test for normality (complete samples). Biometrika 52, 591–611. https://doi.org/10.2307/2333709.

Silva de Souza, L., Landau, L., Moraes, N.O., Pimentel, L.C.G., 2012. Air quality photochemical study over Amazonia Area, Brazil. Int. J. Environ. Pollut. 48, 194–202. https://doi.org/10.1504/IJEP.2012.049666.

Snedecor, G.W., Cochran, W.G., 1989. Statistical Methods, eighth ed. Blackwell Publishing Professional, Ames, Iowa.

Sohngen, B., Beach, R.H., Andrasko, K., 2008. Avoided deforestation as a greenhouse gas mitigation tool. J. Environ. Qual. 37, 1368–1375. https://doi.org/10.2134/jeq2007.0288.

Souto Maior, M.M., Cândido, G.A., 2014. Avaliação das metodologias brasileiras de vulnerabilidade socioambiental como decorrência da problemática urbana no Brasil. Cadernos Metrópole 16, 241–264. https://doi.org/10.1590/2236-9996.2014-3111.

Souza, R.B.D., Stosic, T., 2011. Análise multifractal de séries temporais de focos de calor no Brasil. In: Programa de Pós-Graduação em Biometria e Estatística Aplicada. Universidade Federal Rural de Pernambuco (UFPE).

Souza, L.R., Amanajás, J.C., Silva, A.P.N., Braga, C.C., Correia, M.F., 2011. Determinação de padrões espaço-temporal e regiões homogêneas de precipitação pluvial no estado de Minas Gerais. Eng. Ambient.: Pesquisa e Tecnologia 8 (2).

Souza, M.C., Biudes, M.S., Danelichen, V.H.M., Machado, N.G., Musis, C. R. de, Vourlitis, G.L., Nogueira, J.S., 2014. Estimation of gross primary production of the Amazon-Cerrado transitional forest by remote sensing techniques. Revista Brasileira de Meteorologia 29 (1), 1–12. https://doi.org/10.1590/S0102-77862014000100001.

Tan-Soo, J.S., Pattanayak, S.K., 2019. Seeking natural capital projects: forest fires, haze, and early-life exposure in Indonesia. Proc. Natl. Acad. Sci. Unit. States Am. 116, 5239–5245. https://doi.org/10.1073/pnas.1802876116.

Theisinger, O., Ratianarivo, M.C., 2015. Patterns of reptile diversity loss in response to degradation in the spiny forest of Southern Madagascar. Herpetol. Conserv. Biol. 10, 273–283.

Tomzhinski, G.W., Coura, P.H.F., Fernandes, M.C., 2011. Avaliação da Detecção de Focos de Calor por Sensoriamento Remoto para o Parque Nacional do Itatiaia. Biodiversidade Brasileira 1, 201–211.

Turetsky, M.R., Benscoter, B., Page, S., Rein, G., Van Der Werf, G.R., Watts, A., 2014. Global vulnerability of peatlands to fire and carbon loss. Nat. Geosci. 8, 11–14. https://doi.org/10.1038/ngeo2325.

Van Der Werf, G., Randerson, J.T., Giglio, L., Gobron, N., Dolman, A.J., 2008. Climate controls on the variability of fires in the tropics and subtropics. Global Biogeochem. Cycles 22, 1–13. https://doi.org/10.1029/2007GB003122.

Wan, Z., Hook, S., Hulley, G., 2015. MYD11C3 MODIS/Aqua Land Surface Temperature/Emissivity Monthly L3 Global 0.05Deg CMG V006 [Data set].NASA EOSDIS Land Processes DAAC. https://doi.org/10.5067/MODIS/MYD11C3.006. Accessed 2019-08-19 from.

Westerling, A.L., Gershunov, A., Brown, T.J., Cayan, D.R., Dettinger, M.D., 2003. Climate and wildfire in the western United States. Bull. Am. Meteorol. Soc. 84 (5), 595–604. https://doi.org/10.1175/BAMS-84-5-595.

Wilks, D.S., 2019. Statistical Methods in Atmospheric Sciences, fourth ed. Elsevier, London, p. 807.

WRIBrasil – Os países que mais emitiram gases de efeito estufa nos últimos 165 anos. Disponível em:≤https://wribrasil.org.br/pt/blog/2019/04/ranking-paises-que-mais-emitem-carbono-gases-de-efeito-estufa-aquecimento-global>. Acesso em 10 de setembro de 2019.

Zeri, M., Carvalho, V.S.B., Cunha-Zeri, G., Oliveira-Júnior, J.F., Lyra, G.B., Freitas, E.D., 2016. Assessment of the variability of pollutants concentration over the metropolitan area of São Paulo, Brazil, using the wavelet transform. Atmos. Sci. Lett. 17, 87–95. https://doi.org/10.1002/asl.618.

Zeri, M., Oliveira-Júnior, J.F., Lyra, G.B., 2011. Spatiotemporal analysis of particulate matter, sulfur dioxide and carbon monoxide concentrations over the city of Rio de Janeiro, Brazil. Meteorol. Atmos. Phys. 113, 139–152. https://doi.org/10.1007/s00703-011-0153-9.